研究成果の刊行に関する一覧表

雑誌

発表者氏名	論文タイトル名	発表誌名	巻号	ページ	出版年
Hoshino, A. Iimura, T. Ueha, S. Hanada, S. Maruoka, Y. Mayahara, M. Suzuki, K. Imai, T. Ito, M. Manome, Y. Yasuhara, M. Kirino, T. Yamaguchi, A. Matsushima, K.	Deficiency of Chemokine Receptor CCR1 Causes Osteopenia Due to Impaired Functions of Osteoclasts and Osteoblasts	J Biol Chem	285(37)	28826-28837	2010
Higuchi, Y., Kabasawa, Y., Sato, M., Kikuchi, T., Aoki, K., Ohya, K., Maruoka, Y., Omura, K.	Effect of recombinant human fibroblast growth factor-2 on bone formation in rabbit mandibular distraction models using beta-tricalcium phosphate	Congenital Anomalies	50	95-104	2010
Muto G, Takahashi Y, Yamashita H, Mimori A.	A patient with intravascular lymphoma presenting with cerebral infarction and a high serum MPO-ANCA level	Mod Rheumatol.	Oct 8(E-publish)		2010
Kobayashi M, Takahashi Y, Yamashita H, Kaneko H, Mimori A.	Benefit and a possible risk of tocilizumab therapy for adult-onset Still's disease accompanied by macrophage-activation syndrome	Mod Rheumatol.			2010
Okudaira N, Iijima K, Koyama T, Minemoto Y, Kano S, Mimori A, Ishizaka Y.	Induction of long interspersed nucleotide element-1 (L1) retrotransposition by 6-formylindolo [3,2-b] carbazole (FICZ), a tryptophan photoproduct	Proc Natl Acad Sci U S A.	107	18487-92	2010
Testempassi E, Kubota K, Ito K, Morooka M, Ito K, Masuda-Miyata Y, Yamashita H, Itoh K, Mimori A, Kuriki H.	Conctrictive tuberculoous pericarditis diagnosed using 18F-fluorodeoxy-glucose positron emission tomographu: a report of two cases	Ann Nucl Med.	24(5)	421-425	2010
Takahashi Y, Haga S, Ishizaka Y, Mimori A.	Autoantibodies to angiotensin converting enzyme 2 in patients with connective tissue diseases	Arthritis Res Ther.	12 (3)	R85	2010
Myouzen K, Kochi Y, Shimane K, Fujio K, Okamura T, Okada Y, Suzuki A, Atsumi T, Ito S, Takada K, Mimori A, Ikegawa S, Yamada R, Nakamura Y, Yamamoto K.	Regulatory polymorphisms in EGR2 are associated with susceptibility to systemic lupus erythematosus	Hum Mol Genet.	19 (11)	2313-20	2010
Ito K, Kubota K, Morooka M, Hasuo K, Kuroki H, Mimori A.	Clinical impact of 18F-FDG PET/CT on the management and diagnosis of infectious spondylitis	Nucl Med Commun.	31(8)	691-698	2010
Iimura T, Sugiyama M, Makino Y, Nakane A, Watanabe T and Yamaguchi A.	Illumination of vertebrate development by fluorescence live imaging	Cytometry Research			In print
Iimura T, Himeno A, Nakane A, Yamaguchi A.	Hox genes, a molecular constraint for the development and evolution of the vertebrate body plan	Journal of Oral Biosciences;	52(2)	155-63	2010
Kayamori K, Sakamoto K, Nakashima T, Takayanagi T, Morita K, Omura K, Nguyen ST, Miki Y, Iimura T, Himeno A, Akashi T, Yamada-Okabe H, Ogata E,	Roles of IL-6 and PTHrP in osteoclast formation associated with oral cancers: The significance of IL-6 synthesized by stromal cells in response to cancer cells	Am J Pathol.	176(2)	968-80	2010
Higuchi Y, Kabasawa Y, Sato M, Kikuchi T, Aoki K, Ohya K, Maruoka Y, Omura K.	Effect of recombinant human fibroblast growth factor-2 on bone formation in rabbit mandibular distraction models using beta-tricalcium phosphate	Congenit Anom	50(2)	95-104	2010, E-puboished on Feb. 11
上田 洋、高橋裕子、山下裕之、金子礼志、三森明夫	ループス腎炎に対する免疫抑制治療中に発症し、ボセンタンが有効であったSLE肺動脈性高血圧症の1例	日臨免会誌			印刷中
高橋裕子、越智久さこ、柳井敦、山下裕之、伊藤健司、三森明夫	10年間持続した活動性がTocilizumab治療で寛解した成人発症Still病の1例	日内会誌	99(1)	130-132	2010
飯村忠浩、中根綾子、姫野彰子、杉山真由、山口朗	骨の形態的解析法の進歩:骨のin vivo蛍光イメージングの現状と展望	日本骨形態計測学会雑誌			2010 印刷中
丸岡 豊	第35回日本骨髄腫研究会 特別演題 コメディカルセッション「がん患者さんの口腔ケア」歯科口腔外科の立場から	日本骨髄腫研究会誌	1(1)	36-41	2011
三森明夫	関節リウマチ	Clinical Neuroscience	28(2)	181-183	2010

発表者氏名	論文タイトル名	発表誌名	巻号	ページ	出版年
高橋裕子、三森明夫	ウェジナー肉芽腫の画像	リウマチ科	44(2)	199-203	2010
上田洋、三森明夫	診断力をみがく、イメージトレーニング	内科	106(4)	731-735	2010
三森明夫	膠原病における薬物療法のUp to Date	Nephrology Frontier	9(3)	262-265	2010
三森明夫	ループス腎炎、腎組織と発症時期による治療方針	リウマチ科	44(3)	259-265	2010
三森明夫	多発性筋炎・皮膚筋炎	診断と治療	98(10)	1627-1631	2010
田中良哉、針谷正祥、三森明夫、越智小枝、岸本みつ将	(座談会)関節炎の鑑別	日内会誌	99(10)	2503-2520	2010
Harada H, Omura K	Preoperative concurrent chemotherapy with S-1 and radiotherapy for locally advanced squamous cell carcinoma of the oral cavity: Phase I trial	J Exp Clin Cancer Res.	29	33	2010
Higuchi Y, Kabasawa Y, Sato M, Kikuchi T, Aoki K, Ohya O, Maruoka Y, Omura K	Effect of recombinant human fibroblast growth factor-2 on bone formation in rabbit mandibular distraction models using β-tricalcium phosphate	Congenit Anom.	50(2)	95-104	2010
Hirai H, Omura K, Harada H, Tohara H	Sequential evaluation of swallowing function in patients with unilateral neck	Head Neck.	32(7)	896-904	2010
Kayamori K, Sakamoto K, Nakashima T, Takayanagi H, Morita KI, Omura K, Nguyen ST, Miki Y, Iimura T, Himeno A, Akashi T, Yamada-Okabe H, Ogata E, Yamaguchi A	Roles of interleukin-6 and parathyroid hormone-related peptide in osteoclast formation associated with oral cancers. Significance of interleukin-6 synthesized by stromal cells in response to cancer	Am J Pathol.	176(2)	968-980	2010
Miyazaki H, Omura K, Kakizaki H	Orbital approach via swinging eyelid procedure	Asian J Oral Maxillofac Surg.	22(1)	17-19	2010
Mochizuki Y, Omura K, Kaneoya A, Kayamori K, Yamaguchi A	Osteonecrosis of the mandible associated with bisphosphonate therapy: report of a case with surgical	Oral Surgery	2	153-157	2010
Mochizuki Y, Omura K, Sakamoto K, Nakanishi S, Satoh K, Marukawa E, Yamaguchi A	A case of primary combined neuroendocrine carcinoma with squamous cell carcinoma in the upper	Oral Surg Oral Med Oral Pathol Oral Radiol	109(4)	e34-e39	2010
Mochizuki Y, Omura K, Harada H, Kayamori K, Okada N, Yamaguchi A	Malignant fibrous histiocytoma of the jaws: A report of 3 cases	Asian J Oral Maxillofac Surg.	22(3)	143-147	2010
Prapinjumrune C, Morita K, Kuribayashi Y, Hanabata Y, Shi Q, Nakajima Y, Inazawa J, Omura K	DNA amplification and expression of FADD in oral squamous cell carcinoma	J Oral Pathol Med.	39(7)	525-532	2010
Uekusa M, Omura K, Nakajima Y, Hasegawa S. Harada H, Morita KI, Tsuda	Uptake and kinetics of 5-aminolevulinic acid in oral squamous cell carcinoma	Int J Oral Maxillofac Surg.	39(8)	802-805	2010
小村 健、原田浩之、島本裕彰	遊離血管柄付き骨による下顎再建	日本口腔腫瘍学会誌	22(2)	61-68	2010
北村良平、川元龍夫、宮本 順、樺沢勇司、小村 健、黒原一夫、天笠光雄、森山啓司	馬蹄形骨切り併用Le Fort I 型骨切り術と下顎枝矢状分割術を施行した骨格性下顎前突症例の術後の形態変化	日本顎変形症学会雑誌	20(3)	211-219	2010
栗林悠里、櫻井仁享、伊東大典、小村 健	口腔粘膜に初発した尋常性天疱瘡10例の臨床的検討	日本口腔外科学会雑誌	56(3)	189-193	2010
高 楠旻、櫻井仁享、小村 健	骨破壊を伴った放線菌性下顎骨骨髄炎の1例	日本口腔外科学会雑誌	56(2)	90-94	2010
島本裕彰、小村 健	当科における血管柄つき肩甲骨皮弁による下顎再建	日本口腔腫瘍学会誌	22(4)	122-127	2010
原田浩之、小村 健	上顎歯肉・硬口蓋扁平上皮癌の治療	頭頸部癌	36(4)	383-387	2010
平井秀明、三澤常美、河西八郎、小山敏雄	下唇に発生した血管平滑筋腫の1例口腔領域報告例の臨床病理学的検討	山梨県立中央病院年報	36	67-70	2010
本田 綾、馬場祥行、片岡恵一、鈴木聖一、森田圭一、小村 健、森山啓司	Le Fort I 型骨切り術により幅の広い顎裂を閉鎖した成人片側性口唇口蓋裂の1症例	日本顎変形症学会雑誌	20(3)	258-265	2010
丸川恵理子、吉田文彦、宮崎英隆、櫻井仁享、石井良昌、小村 健	口腔内に初発症状を呈した急性骨髄性白血病の3例	日本口腔外科学会雑誌	56(5)	323-327	2010
森田圭一、菊池 剛、今泉史子、根岸綾子、辻美千子、小村 健	新規創内固定型上顎骨延長装置を用いて治療した両側唇顎口蓋裂術後上顎後退症の1例	日本口腔外科学会雑誌	56(7)	450-454	2010
丸川恵理子、小村 健	骨再生療法に用いる分化・増殖因子および足場の現状(総説)	クインテッセンス・デンタル・インプラントロジー	4	61-70	2010
根岸綾子、尾野雅哉、増田万里、小村健、山田哲司	口腔癌のプロテオーム解析(総説)	病理と臨床	28(5)	506-511	2010

研究成果の刊行に関する一覧表

発表者氏名	論文タイトル名	発表誌名	巻号	ページ	出版年
Shono Y, Ueha S, Wang Y, Abe J, Kurachi M, Matsuno Y, Sugiyama T, Nagasawa T, Imamura M, Matsushima K.	Bone marrow graft-versus-host disease: early destruction of hematopoietic niche after MHC- mismatched hematopoietic stem cell transplantation.	Blood	115(26)	Nov-01	2010

書籍

著者氏名	論文タイトル名	書籍全体の　編集	書籍名	出版社名	出版地	出版年	ページ
三森明夫	疲労、全身倦怠感	金澤一郎、永井良三	今日の診断指針第6版	医学書院	東京	2010年	p15-16
三森明夫	関節リウマチの関節外症状	宮坂信之	関節リウマチ第２版	日本臨床社	東京	2010年	215-217
三森明夫	ガイドライン/治療の手引き	竹内勤	全身性エリテマトーデス、新しい診断と治療の	最新医学	東京	2010年	p229-235
三森明夫	関節穿刺と関節液検査	三森常世	リウマチ膠原病クリニカルスタン	文光堂	東京	2010年	p47-50
三森明夫	Weber-Cristian 病	高久史麿ほか	家庭医学大全科	法研	東京	2010年	p2689-2690
三森明夫	結節性紅斑をきたすリウマチ性疾患	日本リウマチ財団・日本リウマチ	リウマチ病学テキスト	診断と治療社	東京	2010年	p432-435
三森明夫	末梢循環不全	厚労省研究班	混合性結合組織病の治療ガイドライ	厚生労働省	東京	2010年	印刷中

VI. 論 文 別 刷

THE JOURNAL OF BIOLOGICAL CHEMISTRY VOL. 285, NO. 37, pp. 28826–28837, September 10, 2010

Deficiency of Chemokine Receptor CCR1 Causes Osteopenia Due to Impaired Functions of Osteoclasts and Osteoblasts*[S]

Received for publication, December 30, 2009, and in revised form, May 27, 2010 Published, JBC Papers in Press, June 22, 2010, DOI 10.1074/jbc.M109.099424

Akiyoshi Hoshino,[a,b,c1] Tadahiro Iimura,[d2,3] Satoshi Ueha,[e] Sanshiro Hanada,[a] Yutaka Maruoka,[a,f4] Mitsuori Mayahara,[g] Keiko Suzuki,[h] Toshio Imai,[i] Masako Ito,[j] Yoshinobu Manome,[c] Masato Yasuhara,[b] Takaaki Kirino,[k] Akira Yamaguchi,[d2] Kouji Matsushima,[e5] and Kenji Yamamoto[a,b6]

From the [a]International Clinical Research Center, Research Institute, International Medical Center of Japan, Tokyo 162-8655, the [e]Department of Molecular Preventive Medicine, Graduate School of Medicine, The University of Tokyo, Tokyo 113-0033, the Departments of [b]Pharmacokinetics and Pharmacodynamics (Hospital Pharmacy) and [d]Oral Pathology, Global Center of Excellence, Tokyo Medical and Dental University, Tokyo 113-8519, the [c]Department of Molecular Cell Biology, Institute of DNA Medicine, Research Center for Medical Sciences, Jikei University School of Medicine, Tokyo 105-8461, the [f]Department of Dentistry and Oral Surgery, Toyama National Hospital, International Medical Center of Japan, Tokyo 162-8655, the Departments of [g]Oral Histology and [h]Pharmacology, Showa University School of Dentistry, Tokyo 142-8555, the [i]Kan Research Institute, Inc., Kobe 650-0047, the [j]Department of Radiology, Nagasaki University School of Medicine, Nagasaki 852-8501, and the [k]International Medical Center of Japan, Tokyo 162-8655, Japan

Chemokines are characterized by the homing activity of leukocytes to targeted inflammation sites. Recent research indicates that chemokines play more divergent roles in various phases of pathogenesis as well as immune reactions. The chemokine receptor, CCR1, and its ligands are thought to be involved in inflammatory bone destruction, but their physiological roles in the bone metabolism *in vivo* have not yet been elucidated. In the present study, we investigated the roles of CCR1 in bone metabolism using CCR1-deficient mice. *Ccr1*$^{-/-}$ mice have fewer and thinner trabecular bones and low mineral bone density in cancellous bones. The lack of CCR1 affects the differentiation and function of osteoblasts. *Runx2*, *Atf4*, *Osteopontin*, and *Osteonectin* were significantly up-regulated in *Ccr1*$^{-/-}$ mice despite sustained expression of *Osterix* and reduced expression of *Osteocalcin*, suggesting a lower potential for differentiation into mature osteoblasts. In addition, mineralized nodule formation was markedly disrupted in cultured osteoblastic cells isolated from *Ccr1*$^{-/-}$ mice. Osteoclastogenesis induced from cultured *Ccr1*$^{-/-}$ bone marrow cells yielded fewer and smaller osteoclasts due to the abrogated cell-fusion. *Ccr1*$^{-/-}$ osteoclasts exerted no osteolytic activity concomitant with reduced expressions of *Rank* and its downstream targets, implying that the defective osteoclastogenesis is involved in the bone phenotype in *Ccr1*$^{-/-}$ mice. The co-culture of wild-type osteoclast precursors with *Ccr1*$^{-/-}$ osteoblasts failed to facilitate osteoclastogenesis. This finding is most likely due to a reduction in *Rankl* expression. These observations suggest that the axis of CCR1 and its ligands are likely to be involved in cross-talk between osteoclasts and osteoblasts by modulating the RANK-RANKL-mediated interaction.

Chemokines are initially identified as small cytokines that direct the homing of circulating leukocytes into sites of inflammation (1). Chemokines are now recognized to be major factors in inflammation and immune development as well as tumor growth, angiogenesis, and osteolysis. Chemokine receptors are expressed in a well organized spatiotemporal manner in various types of leukocytes, including lymphocytes, granulocytes, and macrophages. They facilitate the recruitment of these cells into inflammatory sites during the appropriate phase of inflammation.

Recent findings indicate that chemokine receptors, including CCR1[7] and its related chemokines, CCL3 and CCL9, are involved in the pathogenesis of a variety of diseases. In particular, CCL3 (also called MIP-1α), a major pro-inflammatory chemokine produced at inflammatory sites, appears to play a crucial role in pathological osteoclastogenesis (2, 3). In osteolytic bone inflammation (*e.g.* rheumatoid arthritis-associated bone destruction), CCL3 induces ectopic osteoclastogenesis (4)

* This work was supported in part by Grant H19-nano-012 from the Ministry of Health, Labor and Welfare (to K. Y.) and by a research fellowship from the Japan Society for the Promotion of Science for Young Scientists (2007–2009) (to A. H.).

[S] The on-line version of this article (available at http://www.jbc.org) contains supplemental Figs. 1–3.

[1] Supported by grants from the Japan Foundation of Cardiovascular Research (2006) and from the Naito Foundation (2005).

[2] Supported by a grant from the Japanese Ministry of Education, Global Center of Excellence Program, International Research Center for Molecular Science in Tooth and Bone Diseases.

[3] Supported by The Takeda Science Foundation, The Mochida Memorial Foundation for Medical and Pharmaceutical Research, and a Grant-in-Aid for Scientific Research from the Japan Society for the Promotion of Science (21659426).

[4] Supported by Grants H21-nanchi-097 and H22-nanchi-ippan157 from the Ministry of Health, Labor and Welfare.

[5] Supported by Solution Oriented Research for Science and Technology and by Japan Science and Technology Corp.

[6] To whom correspondence should be addressed: International Clinical Research Center, Research Institute, International Medical Center of Japan, Toyama 1-21-1, Shinjuku-ku, Tokyo 162-8655, Japan. Tel.: 81-3-3202-7181 (ext: 2856 or 5611); E-mail: backen@ri.ncgm.go.jp.

[7] The abbreviations used are: CCR, C-C chemokine receptor; M-CSF, macrophage-colony stimulation factor; BALP, bone-specific alkaline phosphatase; CCL, C-C chemokine ligand; MCP-1, macrophage chemoattractant protein-1; MIP-1, macrophage inflammatory protein-1; CT, computed tomography; PTX, pertussis toxin from *Bordetella pertussis*; RANK, receptor activator of NF-κB; RANKL, receptor activator of NF-κB ligand; RANTES, regulated upon activation normal T expression and secreted; TRAP, tartrate-resistant acid phosphatase; NTx, N-telopeptides.

and results in bone destruction (5). Several reports suggested that CCL3 is also produced by myeloma cells and directly stimulates bone destruction in myeloma-related bone diseases (5–7). These findings indicate the possible roles of CCL3 as a crucial chemokine for osteoclast function. Several antagonists of the chemokine ligands of CCL3, such as CCR1-specific (BX471) and CCR5-specific (TAK779) blockers, have been tested as drug candidates for the treatment of patients with rheumatoid arthritis-associated bone destruction and multiple myeloma (4, 8). The chemokine CCL9 (also called MIP-1γ), is also abundantly produced by various myeloid lineage-derived cells, including osteoclasts (9), activates osteoclastogenesis through its receptor, CCR1 (10–12). However, the exact physiological functions of CCR1 and its related chemokines in bone remodeling are still not fully characterized (12, 13).

A recent study using an ovariectomy-induced bone loss model found that the chemokine receptor CCR2 was associated with postmenopausal bone loss (14), but there are few reports on bone phenotypes in other chemokine receptor-deficient mouse models. In the present study, we demonstrated that osteopenia in *Ccr1*$^{-/-}$ mice appeared to be due to impaired osteoclast and osteoblast function. Our data also uncovered a possible role for CCR1 and its related ligands in the communication between osteoclasts and osteoblasts.

EXPERIMENTAL PROCEDURES

Mice—Standard male C57BL/6 mice (6–9 weeks of age) were obtained from CLEA Japan. *Ccr1*$^{-/-}$ mice (15) purchased from Jackson Laboratories were backcrossed for 8–10 generations on the C57BL/6 background mice. Mice were all bred and maintained under pathogen-free conditions at the animal facilities of the University of Tokyo. All experiments were performed according to the Institutional Guidelines for the Care and Use of Laboratory Animals in Research and were approved by the ethics committees of both the University of Tokyo and the Research Institute of International Medical Center of Japan.

Materials—Recombinant mouse M-CSF and RANKL were purchased from R&D Systems Inc. (Minneapolis, MN) and PeproTech Inc. (Rocky Hill, NJ), respectively. Recombinant mouse CCL2 (MCP-1), CCL3 (MIP-1α), CCL4 (MIP-1β), CCL5 (RANTES), CCL9 (MIP-1γ), and CCL11 (eotaxin-1) and their corresponding-neutralizing antibodies were purchased from R&D Systems. Control rat IgG was purchased from Jackson ImmunoResearch (Bar Harbor, ME). Recombinant mouse CX3CL1 (fractalkine) was purchased from R&D Systems. Hamster anti-CX3CL1-neutralizing antibody and control hamster IgG were kindly provided by Dr. Toshio Imai (Kan Research Institute, Kobe, Japan). Rabbit anti-human/mouse CCR1 polyclonal antibody and control rabbit IgG were purchased from AbCam (Cambridge, MA) and Chemicon (Temecula, CA), respectively. Secondary antibodies (Alexa488-labeled anti-rabbit IgG and Streptavidin-PE) were purchased from Molecular Probes (Eugene, OR). Rabbit anti-TRAP and anti-Cathepsin K polyclonal antibodies were both purchased from Santa Cruz Biotechnology (Santa Cruz, CA).

Osteoclast and Osteoblastic Cell Culture—Mouse bone marrow cells cultured in α-minimal essential medium were used as sources of osteoclastic and osteoblastic cell cultures. The non-adherent cells were collected for bone marrow-derived macrophage and pre-osteoclast induction, and adherent bone marrow-derived mesenchymal stromal cells were collected for osteoblast induction. Bone marrow-derived macrophages were induced with 10 ng/ml M-CSF for an additional 10 days. To generate pre-osteoclasts, non-adherent cells were passed through a column filled with Sephadex G-10 microspheres (Amersham Biosciences) and were then cultured with 10 ng/ml M-CSF and 20 ng/ml RANKL for 4 days. The mature osteoclasts were induced from pre-osteoclasts by culturing for an additional 14 days with M-CSF and RANKL. The culture media were replaced every 3 days. TRAP activity in the osteoclasts was determined by staining using an acid phosphatase leukocyte staining kit (Sigma). The contamination of stromal/osteoblastic cells was monitored using Q-PCR analysis, as a low expression level of the *Osteoprotegrin* gene indicates stromal/osteoblastic cells.

Osteoblastic differentiation in adherent bone marrow mesenchymal stromal cells was induced by culture in α-minimal essential medium containing 10% FBS, 200 μM ascorbic acid, 10 mM β-glycerophosphate, and 10 nM dexamethasone (16). The culture media was replaced once every 3 days in the presence or absence of chemokine-neutralizing antibodies. The cells were fixed with 4% paraformaldehyde and stained for alkaline phosphatase with naphthol AS-MX phosphate plus Fastblue-BB (Sigma) and for minerals with alizarin red. Mineral deposition was alternatively identified by von Kossa staining (Polysciences, Inc., Warrington, PA), and the mineralized areas were measured by using an Array Scan VTI HCS analyzer (Beckman Coulter).

Co-culture experiments with osteoclast precursors and osteoblasts were performed by inoculating bone marrow-derived precursors (1×10^5 cells/well) onto the layer of osteoblastic cells that had been cultured for 21 days with osteoblast-inducing media in 24-well plates. Thereafter, these cells were co-cultured for 7 days in α-minimal essential medium supplemented with 10% FBS and 10 μg/ml vitamin D_3. To assess bone resorption activity, these co-culture studies were also conducted using bone slices. After fixation of the cells with 2.5% glutaraldehyde/1.6% paraformaldehyde in 0.1 M cacodylic acid (pH 7.4), the bone slices were briefly rinsed, and were completely dehydrated in an ascending series of ethanol and liquid carbon dioxide. The samples were coated with an ultrafine titanium oxide powder and observed under a scanning electron microscopy.

Immunohistochemical Staining—For the immunohistochemical staining analyses, osteoclasts were fixed with 4% paraformaldehyde, permeabilized, and stained with the indicated specific antibodies, followed by Alexa594-conjugated secondary antibodies and Alexa488-labeled phalloidin (Molecular Probes). The osteoclasts with multiple nuclei (>3) were quantified. Images were captured using an IX-81 fluorescence microscope equipped with a confocal microscopy DSU unit (Olympus, Japan) and were analyzed with the MetaMorph™ software program (Universal Imaging, Molecular Devices, Sunnyvale, CA). The formation of osteoclasts was quantified by capturing and analyzing images using the ImageJ software program (National Institutes of Health, Bethesda, MD) based on

TRAP staining of 25 fields in each well, which were randomly chosen and analyzed.

Real-time PCR Analysis—Total cellular RNA from osteoclasts, osteoblasts, and bone tissues (proximal tibia after the bone marrow flush and the removal of metaphysial regions) was isolated using the RNeasy kit (Qiagen, Valencia, CA). The total RNA was then reverse-transcribed into cDNA using the Superscript III RT kit (Invitrogen). The real-time quantitative PCR analyses were performed using the ABI 7700 sequence detector system with SYBR Green (Applied Biosystems, Foster City, CA). The sequences were amplified for 40 cycles under the following conditions: denaturation at 95 °C for 15 s, annealing at 60 °C for 30 s, and extension at 72 °C for 45 s with primers for the chemokine receptors as previously reported (17). Gene expression levels were compared with *Gapdh* gene expression by the $2^{-\Delta(Ct)}$ method.

Measurement of Cytokines and Chemokines—Chemokine CCL5 and CCL9 secretion levels were determined by ELISA using the antibodies MAB4781 and BAF478 (R&D systems) and MAB463 and BAF463 (R&D systems), respectively. The reaction intensities were determined by using HRP-conjugated streptavidin (Chemicon). The cytokine production levels were quantified with a mouse 23-plex multiple cytokine detection system (Bio-Rad Corp., Hercules, CA) according to the manufacturer's instructions.

Flow Cytometry—FITC-, PE-, APC-, PerCP-Cy5.5-, PE-Cy7-, or biotin-conjugated anti-mouse mAbs to CD45.2 (104), CD115 (AFS98), and CD265/RANK (R12–31), and subclass-matched control antibodies were purchased from eBioscience (San Diego, CA). Anti-mouse mAbs to FcγR (2.4G2), Ly6C/6G (RB6 – 8C5), CD11b (M1/70), and CD19 (1D3) were purchased from BD Pharmingen (San Diego, CA). The flow cytometric analyses were performed using an LSR II flow cytometer with the FACS diva software program (BD Biosciences) and were analyzed with the FlowJo software program (TreeStar, Ashland, OR). Dead cells were excluded on the basis of the forward and side scatter profiles and propidium iodide staining.

Microcomputed Tomography and Peripheral Quantitative Computed Tomography—Micro-computed tomography (microCT) scanning was performed on proximal tibiae by μCT-40 (SCANCO Medical AG) with a resolution of 12 μm, and the microstructure parameters were three-dimensionally calculated as previously described (18). The bone scores were measured by peripheral quantitative CT using the XCT Research SA+ system (Stratec Medizintechnik GmbH, Pforzheim, Germany). The bone scores and density were measured and analyzed at 1.2 mm below the epiphyseal plate of distal femora. The scores were defined according to the American Society for Bone and Mineral Research standards.

Bone Histomorphometry—The unilateral proximal tibiae fixed with ethanol were embedded in glycol methacrylate, and the blocks were cut in 5-μm-thick sections. The structural parameters were analyzed at the secondary spongiosa. For the assessment of dynamic histomorphometric indices, calcein (at a dose of 20 mg/kg body weight) was injected twice (72-h interval) to wild-type and *Ccr1*-deficient mice, respectively. The sections were stained with toluidine blue and analyzed using a semi-automated system (Osteoplan II, Zeiss). The nomenclature, symbols, and units used in the present study are those recommended by the Nomenclature Committee of the American Society for Bone and Mineral Research (19).

Measurement of TRAP, BALP, and Collagen-type I N-telopeptides (NTx)—Tartrate-resistant acid phosphatases (TRAP5b) in serum and culture supernatant were measured by the mouse TRAP EIA assay kit (Immunodiagnostic system, Fountain Hills, AZ). In brief, the culture supernatant or diluted serum was applied to an anti-TRAP5b-coated microplate, according to the manufacturer's instruction. The enzymatic activities of bound TRAP were determined with chromogenic substrates. Bone-specific alkaline phosphatase (BALP) levels were measured using the mouse BALP ELISA kit (Cusabio Biotech Co. Ltd., Wilmington, DE). Collagen-type I NTx were measured by ELISA (SRL, Tokyo).

Collagen-based Zymography—Collagen digestion activity was measured by using modified methods, which were based on gelatin-based zymography (20), with some modification for type-I collagen (21, 22). In brief, the osteoclasts were gently digested with lysis buffer (150 mM NaCl, 50 mM HEPES, 5 mM EDTA, and 10% Nonidet P-40 with Halt protease inhibitor mixture, pH 7.5). The lysates were separated by SDS-PAGE on a 10% polyacrylamide gel with porcine type-I collagen (1 mg/ml, Nitta Gelatin Inc., Osaka, Japan) under chilled conditions. The gel was washed with denaturation buffer (Tris-buffered saline (150 mM NaCl, 25 mM Tris-HCl, pH 7.4, supplemented with 2.5% Triton X-100) and then subjected to zymography for 18–24 h at 37 °C in zymography developing buffer (Tris-buffered saline, supplemented with 1 mM $CaCl_2$, 1 μM $ZnCl_2$, and 0.05% Brij-35). The signals were detected using Coomassie Brilliant Blue solution (Wako Pure Chemicals, Osaka, Japan).

Immunoblot Analysis—Total cell lysates were isolated, separated by SDS-PAGE, and electrotransferred onto Immobilon-P PVDF membranes (Millipore). The membrane was blocked by 5% BSA in TBST (150 mM NaCl, 25 mM Tris-HCl (pH 7.4) supplemented with 0.1% Tween 20) and incubated with rabbit anti-ATF4 polyclonal antibody (1/2,000), followed by HRP-conjugated anti-rabbit IgG (1/10,000). The signals were detected using an ECL chemiluminescence substrate (Amersham Biosciences). The quantitative analysis of blots was normalized using the lumino image analyzer LAS-4000 (Fujifilm Corp., Japan).

Statistics—Data are presented as the mean ± S.E. for the indicated number of independent experiments. Statistical significance was determined with a post-hoc test of one-factor factorial analysis of variance (Figs. 3*E*, 6*D*, 7*B*, and 7*C*), the Wilcoxon Mann-Whitney *U* test (non-parametric analysis, Fig. 2*C*, and Fig. 6*C*), and Student's *t* test (other figures) using the KaleidaGraph® 4.0 programs (Synergy Software, Reading, PA). Differences with a p value of <0.05 was considered statistically significant (* and # indicate up-regulation and down-regulation, respectively; NS indicates not significant).

RESULTS

CCR1-deficient Mice Exhibit Osteopenia—To understand the functions of CCR1 in bone metabolism, we investigated the bone mineral density in $Ccr1^{-/-}$ mice. A peripheral quantitative CT analysis showed a significant reduction in bone mineral

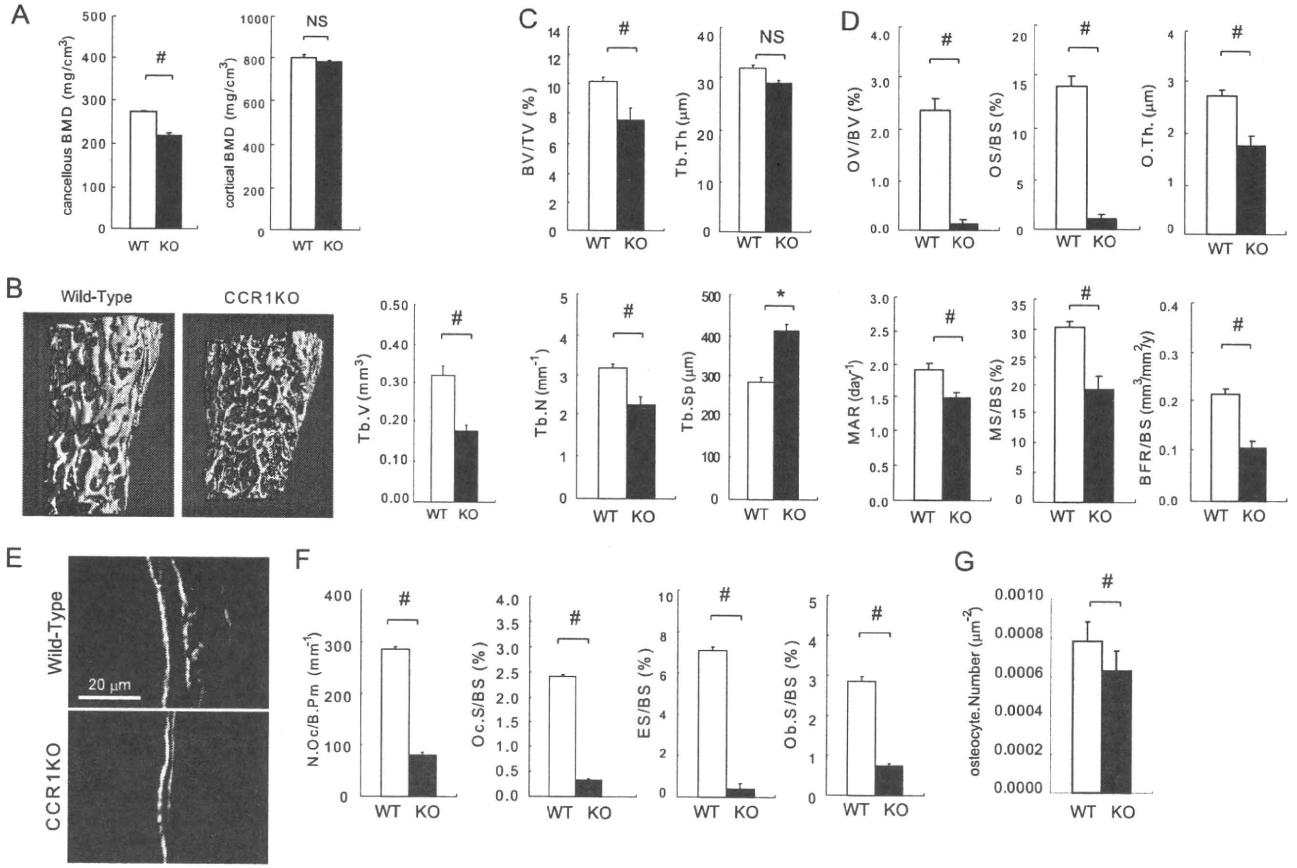

FIGURE 1. **Bone morphometric analyses of CCR1$^{-/-}$ mice.** *A* shows the bone mineral density of trabecular and cortical bones in distal femurs as measured by peripheral quantitative CT. *B* shows the microCT images and the quantitative measurements of trabecular bones (*Tb.V.*) in the distal femurs of wild-type and *Ccr1*$^{-/-}$ mice (n = 10). In *C–F*, the bone histomorphometric analyses of distal femurs in wild-type and *CCR1*$^{-/-}$ mice were carried out as described under "Experimental Procedures." Parameters relating to the trabecular structure (in *C*): bone volume per tissue volume (*BV/TV*), trabecular number (*Tb.N.*), and trabecular separation (*Tb.Sp.*). Parameters relating to bone formation (in *D*): osteoid volume to bone volume (*OV/BV*), osteoid surface/bone surface (*OS/BS*), osteoid thickness (*O.Th.*), formation rate referenced to bone surface (*BFR/BS*), mineral apposition rate (*MAR*), and mineralizing surface per bone surface (*MS/BS*). The immunofluorescence images of calcein labeling in wild-type and *Ccr1*$^{-/-}$ mice (in *E*). Parameters relating to bone resorption (in *F*): osteoclast number per bone perimeter (*N.Oc./B.Pm*), osteoclast surface per bone surface (*Oc.S./BS*), eroded surface per bone surface (*ES/BS*), and osteoblast surface per bone surface (*Ob.S./BS*). The bone histomorphometric analysis data are represented as the mean ± S.E. obtained from six mice in each group. #, significantly different from wild-type controls, $p < 0.05$. In *G*, osteocyte numbers per area are represented as the mean ± S.E. obtained from three mice in each group.

density in cancellous bone in *Ccr1*$^{-/-}$ mice compared with wild-type mice (Fig. 1*A*). There were no significant differences between bone mineral density in the cortical bone at the metaphysial (Fig. 1*A*) and diaphysial regions (data not shown) between *Ccr1*-deficient and wild-type mice. In *Ccr1*$^{-/-}$ mice, a microCT analysis indicated decreased cancellous bone tissue at the metaphysical region (Fig. 1*B*). An analysis of bone histomorphometrics confirmed a significant decrease of bone volume (*BV/TV*) at the metaphysial region of *Ccr1*$^{-/-}$ mice. This was associated with a diminished number of trabeculae (*Tb.N*), increased trabecular bone separation (*Tb.Sp*), and no significant changes in trabecular bone thickness (*Tb.Th*), thus indicating that *Ccr1*-deficient mice have sparse trabeculae (Fig. 1*C*). We examined the effect of *Ccr1* deficiency on the function of osteoblasts and osteoclasts in bone morphometry (Fig. 1, *D–F*). The morphological analyses revealed that *Ccr1*$^{-/-}$ mice have a significantly reduced number of osteoblasts (*Ob.S./BS*) (Fig. 1*F*). *Ccr1*$^{-/-}$ mice exhibited extremely low values of osteoid surface (*OS/BS*) and osteoid volume (*OV/BV*) compared with wild-type mice (Fig. 1*D*). Notably, *Ccr1*$^{-/-}$ mice showed a significant decreases in the mineral apposition rate (*MAR*), mineralized surface (*MS/BS*), and bone formation rate (*BFR/BS*) (Fig. 1*D*), which were calculated based on calcein administration (*representative pictures* are shown in Fig. 1*E*). In addition, the number of osteocytes per area was significantly reduced in *Ccr1*$^{-/-}$ mice (Fig. 1*G*). These results indicate that *Ccr1*$^{-/-}$ mice have impaired bone formation. Fig. 1*F* summarizes the bone morphometric parameters associated with bone resorption. *Ccr1*$^{-/-}$ mice have significantly decreased osteoclast numbers (*N.Oc./B.Pm*) and osteoclast surface area (*Oc.S./BS*), and an eroded surface (*ES/BS*). These findings indicate that *Ccr1*$^{-/-}$ mice have diminished osteoclast function. Taken together, the morphometric analyses suggest that the bone phenotype in *Ccr1*-deficient mice exhibit osteopenia with low bone turnover, which is most likely due to the diminished function of osteoblasts and osteoclasts.

Impaired Osteogenesis and Osteoclastogenesis in the Bone Tissue of Ccr1-deficient Mice—To elucidate the status of osteoblasts and osteoclasts in bones of *Ccr1*$^{-/-}$ mice, we compared the transcriptional levels of osteoclast- and osteoblast-related

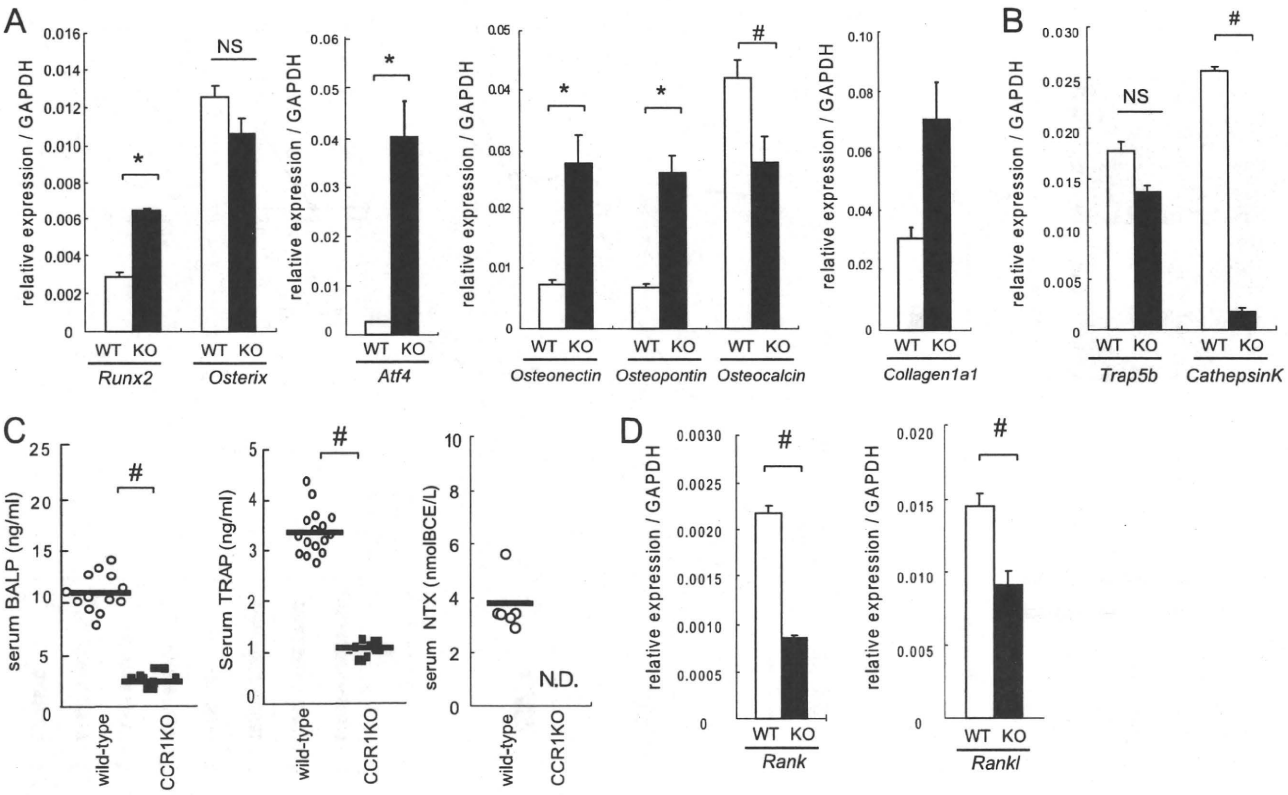

FIGURE 2. **Expression of markers related to osteoblasts and osteoclasts in bones and sera in wild-type and *CCR1*$^{-/-}$ mice.** In *A*, *B*, and *D*, total RNAs were isolated form the proximal tibia of wild-type and *Ccr1*$^{-/-}$ male mice at 8 weeks of age. Real-time Q-PCR revealed the relative expression levels of osteoblast-related mRNAs (*Runx-2*, *Osterix*, *Atf4*, *Osteonectin*, *Osteopontin*, *Osteocalcin*, and *Collagen1α1*, *A*), osteoclast-related mRNA (*Trap5a* and *Cathepsin K*, *B*), and RANK–RANKL axis (*Rank* and *Rankl*, *D*). Data are expressed as the copy numbers of these markers normalized to *Gapdh* expression (mean ± S.E., $n = 8$). In *C*, the levels of serum BALP, TRAP, and *serum* collagen-type1 N-telopeptides (*NTx*) were measured by ELISA. The *bars* indicate the mean ± S.E. Each sample was duplicated. Wild-type and *Ccr1*$^{-/-}$ male mice at 9 weeks of age ($n = 10$ and 6, respectively) were subjected to BALP and TRAP. Wild-type and *Ccr1*$^{-/-}$ male mice at 9–13 weeks of age ($n = 8$ and 6, respectively) were assayed for NTx. #, significantly different from wild-type controls, $p < 0.05$. *N.D.*, not detected.

markers in the proximal tibiae of wild-type and *Ccr1*$^{-/-}$ mice. The analyses of osteoblast-related markers, such as bone-specific transcriptional factors (*Runx-2*, *Atf4*, and *Osterix*) (23–25) and bone matrix proteins (*Collagen1a1*, *Osteonectin*, *Osteopontin*, and *Osteocalcin*), revealed that the expression levels of *Runx2* and *Atf4* were dramatically up-regulated in *Ccr1*$^{-/-}$ mice than in wild-type mice (Fig. 2*A*). However, there were no significant changes in the expression levels of *Osterix*. Early markers for osteoblast differentiation, including *Collagen1a1*, *Osteonectin*, and *Osteopontin*, were significantly up-regulated. *Osteocalcin* expression, a marker for mature osteoblasts, was significantly down-regulated in *Ccr1*$^{-/-}$ mice. These results suggest that osteoblasts in *Ccr1*-deficient mice are retained in an immature state due to the overexpression of *Runx-2* and *Atf4* by osteoblasts, which is also consistent with the significant reduction in number of osteocytes in *Ccr1*$^{-/-}$ mice. Constitutive *Runx-2* overexpression in osteoblasts results in maturation arrest in osteoblasts and in a reduced number of osteocytes (25). The serum levels of BALP in *Ccr1*-deficient mice were significantly decreased (Fig. 2*C*).

The expression levels of markers related to osteoclast differentiation, revealed attenuated transcription levels of *TRAP5b* and *cathepsin K* in *Ccr1*$^{-/-}$ mice (Fig. 2*B*). In addition, *Ccr1*$^{-/-}$ mice exhibited significantly decreased levels of serum TRAP (26) and collagen-type I *NTx* (*27, 28) (Fig. 2C*). This finding is consistent with diminished osteoclastic bone resorption in *Ccr1*$^{-/-}$ mice. These observations led us to assess the RANK-RANKL axis, a key signaling pathway in osteoblast-osteoclast interactions that regulates osteoclast differentiation and function. Interestingly, the analyses revealed that both *Rank* and *Rankl* were down-regulated (Fig. 2*D*), thus implying that CCR1 is involved in the regulation of the RANK-RANKL axis. Considering the fact that *Ccr1*$^{-/-}$ mice exhibit osteopenia with low bone turnover, these bone cell marker expression levels suggest that CCR1 is heavily involved in the differentiation and function of osteoblasts and osteoclasts as well as in the cellular interactions between these cell types.

CCR1 Signaling Is Important in the Maturation and Function of Osteoblasts—To further corroborate the necessity of CCR1 in osteoblast maturation and function, we examined the formation of mineralized nodules *in vitro* by osteoblastic cells isolated from bone marrow of wild-type and *Ccr1*$^{-/-}$ mice. Mineralized nodule formation in osteoblastic cells isolated from *Ccr1*$^{-/-}$ mice was markedly abrogated compared with wild-type osteoblastic cells (Fig. 3*A*). We next investigated the time-course expression profiles of osteoblastic markers in this *in vitro* culture system and compared them between wild-type and *Ccr1*$^{-/-}$ mice (Fig. 3*B*). In wild-type mice, *Runx2* exhibited the highest levels of expression at day 14, but was drastically down-regulated at day 21, during the mineralization stage. However,

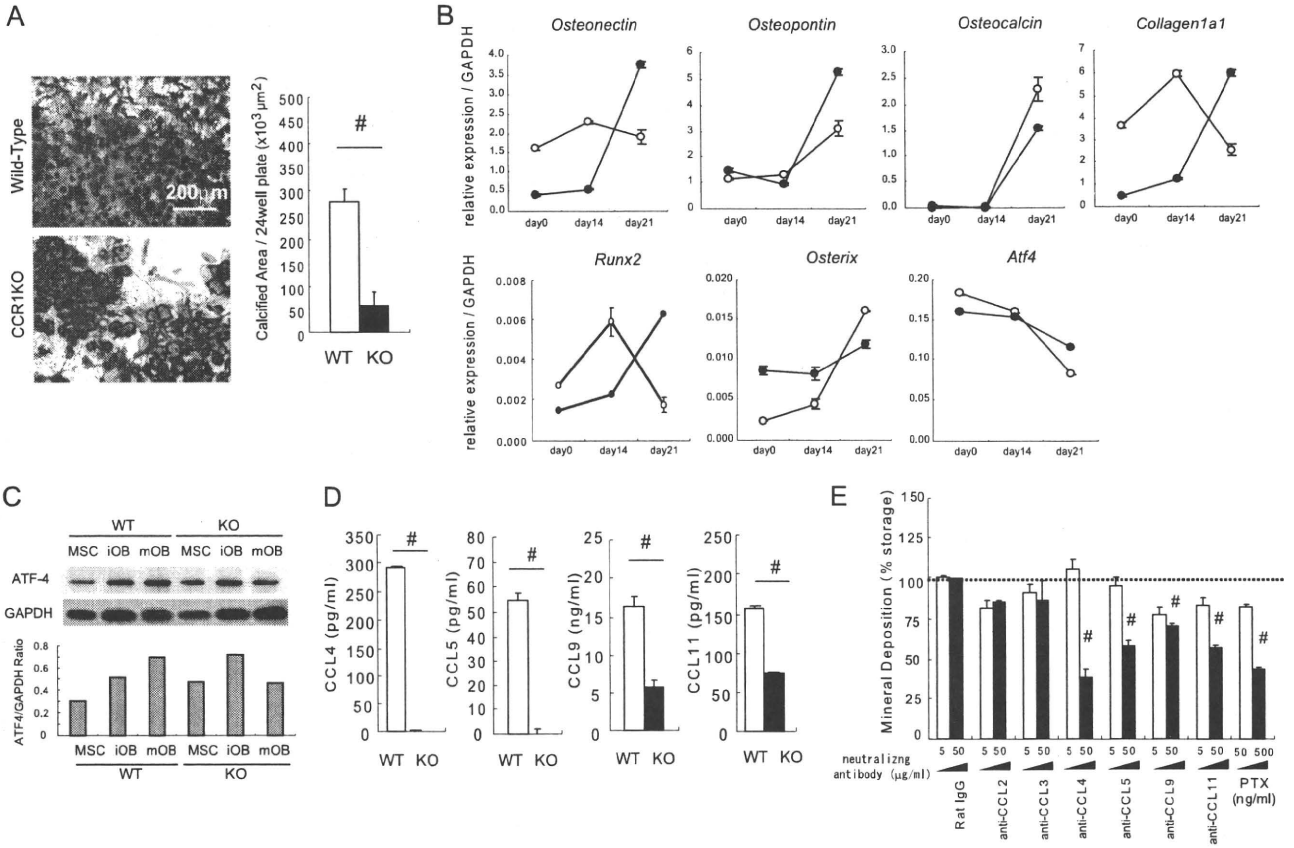

FIGURE 3. **Impaired mineralized nodule formation in *CCR1*-deficient osteoblastic cells.** In *A*, osteoblastic cells were cultured from the bone marrow of wild-type and *Ccr1*$^{-/-}$ mice, and then minerals were stained with alizarin red and BALP with chromogenic reagents (shown in "*blue*") (magnification ×100, *left*). Mineral deposition was determined by von Kossa staining ($n = 6$, *right*). In *B*, total RNAs were isolated from osteoblastic cells isolated from wild-type (*open circles*) and *Ccr1*$^{-/-}$ mice (*filled circles*). The real-time Q-PCR analyses examined the relative expression levels of osteoblast-related transcriptional factor mRNAs (*Runx-2*, *Osterix*, and *Atf4*) and osteoblast-related marker mRNAs (*Osteonectin*, *Osteopontin*, *Osteocalcin*, and *Collagen1α1*). Data are expressed as the copy numbers of these markers normalized to *Gapdh* expression (mean ± S.E., $n = 8$). In *C*, the protein expression levels of the transcriptional factor ATF4 by wild-type and *Ccr1*$^{-/-}$ osteoblastic cells were measured by a Western blot analysis. Osteoblast lysates (10 μg of protein per lane) was loaded and separated by SDS-PAGE. The expression levels of ATF4 were normalized to GAPDH expression. In *D*, the production of CCR1-related chemokine ligands in the culture media of wild-type and *Ccr1*$^{-/-}$ osteoblastic cells was measured by ELISA ($n = 5$). #, significantly different from wild-type controls, $p < 0.05$. In *E*, osteoblastic cells were cultured with the indicated neutralizing antibodies against chemokines. The mineral deposition rate was measured by von Kossa staining ($n = 4$). Stained cells cultured with control rat IgG were set as 100%. #, significantly different from between different concentrations of each antibody, $p < 0.05$. *PTX*, pertussis toxin.

an inverse *Runx2* expression pattern was observed in CCR1-deficient osteoblastic cells, in which the levels of expression were markedly suppressed in the early stages (days 0 and 14), and was then significantly up-regulated at day 21, reaching the levels present in wild-type mice. *Osterix* expression was highly up-regulated at day 21 in wild-type mice, whereas its expression in CCR1-deficient osteoblastic cells was sustained at an intermediate level between the lowest and the highest levels in wild-type mice, overall resulting in a lower expression levels than in wild-type mice at day 21. These inverted expression patterns were also consistently observed, especially at day 21, with other osteoblastic markers, including *Atf4*, *Caollagen1a1*, *Osteonectin*, *Osteopontin*, and *Osteocalcin*. Similarly, the expression pattern of ATF4 was also confirmed by a Western blot analysis (Fig. 3*C*). These observations indicated that CCR1 deficiency severely affected the temporal expression of osteoblastic markers, resulting in the impaired differentiation and maturation of osteoblasts. Because CCR1 signaling is activated by several cross-reactive chemokines (CCL4, CCL5, CCL9, and CCL11), we next compared the levels of these chemokines in wild-type and CCR1-deficient osteoblastic cells. We observed significantly diminished expression levels of these chemokines in *CCR1*-deficient osteoblastic cells (Fig. 3*D*). A test on the effects of neutralizing antibodies against various chemokines, including CCR1 ligands, revealed the role of each chemokine in mineralized nodule formation by osteoblastic cells. The neutralizing antibodies against CCL4, CCL5, CCL9, and CCL11 significantly reduced the number of mineralized nodules in osteoblastic cells, although the antibodies against CCL2 and CCL3 did not inhibit the numbers completely (Fig. 3*E*). Pertussis toxin (PTX), an inhibitor of G_i protein-coupled receptors involved in chemokine signaling, inhibited mineralized nodule formation in a dose-dependent manner. In further support of these findings, we observed similar temporal changes in the transcriptional levels of osteoblastic markers in wild-type osteoblastic cultures treated with an anti-CCL9 antibody, compared with *Ccr1*$^{-/-}$ osteoblastic cells (supplemental Fig. 2). These results suggest that CCR1 signaling mediated by its ligands (CCL4, CCL5, CCL 9, and CCL11) plays an essential role in mineralized nodule formation.

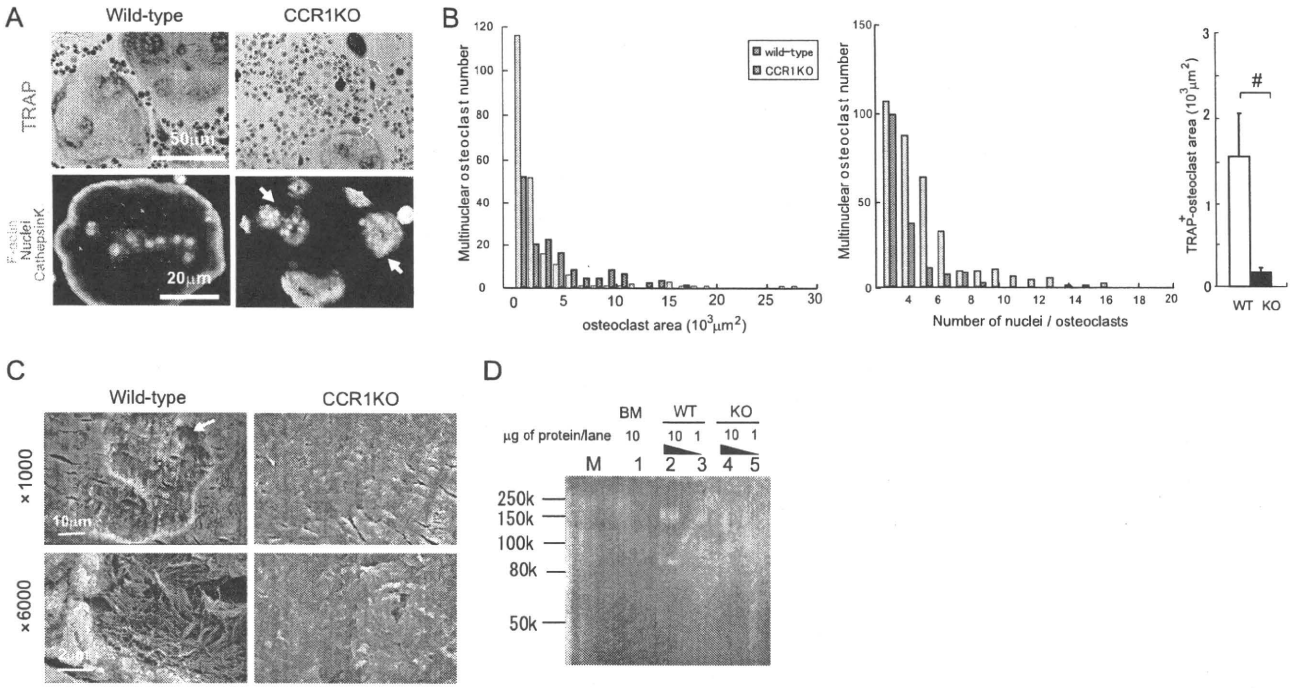

FIGURE 4. **Essential roles of CCR1 in multinucleation and bone-resorbing activity.** Pre-osteoclastic cells were cultured from the bone marrow of wild-type and *Ccr1*$^{-/-}$ mice. Osteoclasts were induced from the pre-osteoclastic cells by M-CSF and RANKL treatment. In *A*, the formation of multinuclear osteoclasts by wild-type and *Ccr1*$^{-/-}$ precursors was visualized by TRAP chromogenic staining (magnification ×400, *upper panels*). Immunohistochemical staining was carried out using an anti-cathepsin K antibody conjugated with Alexa594 (*red*). F-actin and nuclei were counterstained by phalloidin-AlexaFluor 488 (*green*) and Hoechst 33258 (*blue*), respectively (magnification ×640, *bottom panels*). The *yellow arrow* indicates multinuclear giant cells with an impaired actin ring rearrangement, and the *red arrows* indicate TRAP accumulation. In *B*, *histograms* of the area distribution of multinuclear osteoclasts delimited with phalloidin, and of the number of multinuclear osteoclasts in *A*. Area comprises TRAP-positive multinuclear (>3 nuclei) giant cells shown in *A* (mean ± S.E., $n = 3$). In *C*, pit formation by wild-type and *Ccr1*$^{-/-}$ osteoclasts on bone slice observed by scanning electron microscopy (magnification: ×1000 (*top*) and ×6000 (*bottom*), respectively). In *D*, collagen digestion activity by wild-type and *Ccr1*$^{-/-}$ osteoclasts was measured by collagen-based zymography. *Lanes M*, *1*, *2–3*, and *4–5* indicate the molecular markers, bone marrow-derived macrophage lysates (10 μg of protein/*lane*), wild-type osteoclast lysates (1 and 10 μg of protein/*lane*), and *Ccr1*$^{-/-}$ osteoclasts lysates (1 and 10 μg of protein/each *lane*), respectively.

Lack of Chemokine Receptor CCR1 Causes Impaired Osteoclast Differentiation and Bone-resorbing Activity—To elucidate the roles of CCR1 in osteoclast differentiation, we analyzed the differentiation potency of osteoclast precursors derived from *Ccr1*$^{-/-}$ mice (Fig. 4*A*). Osteoclast precursors from *Ccr1*-deficient mice markedly abrogated multinucleation with defective actin ring formation (Fig. 4*A*, *yellow arrows*) compared with precursors from wild-type mice, which generated a large numbers of osteoclasts with multinucleation and well organized actin ring formation at the cell periphery. The histograms of the osteoclast area and number of nuclei per cell as well as TRAP-positive areas reveal the presence of impaired cellular fusion and differentiation in *Ccr1*-deficient osteoclasts (Fig. 4*B*). We further investigated the activity of bone resorption in *Ccr1*-deficient osteoclasts (Fig. 4*C*). Few resorption pits were observed in *Ccr1*$^{-/-}$ osteoclasts by scanning electron microscopic examination, in contrast to obvious resorption pits with well digested collagen fibers detected in wild-type osteoclasts. This observation was also confirmed by collagen zymography demonstrating that *Ccr1*$^{-/-}$ osteoclasts failed to digest type-I collagens (Fig. 4*D*).

Furthermore, the transcriptional levels of osteoclastic differentiation markers were investigated in the osteoclast culture system. *Rank* and its downstream targets *Nfat-c1*, other markers such as *c-fos*, *Trap*, *CathepsinK*, *Atp6v0d2*, *integrin αV*, and *integrin β3* were markedly down-regulated in *Ccr1*-deficient cells, whereas *S1P*$_1$ and *Irf-8* were up-regulated (Fig. 5*A*). We next examined whether the down-regulation in RANK expression *in vivo* (see Fig. 2*D*) and *in vitro* (Fig. 5*A*) directly correlated with the reduction in RANK-expressing osteoclast precursors. The cellular profiles of osteoclast precursors by a flow cytometric analysis revealed that the *Ccr1*$^{-/-}$ mice had lower numbers of CD45$^+$CD11b$^+$CD115$^+$ myeloid-lineage precursors compared with wild-type mice (Fig. 5*B*). In addition, the subpopulations of osteoclast precursors, which are categorized into CD11b^{hi} (R1) and CD11b^{lo} (R2), were marked reduced in the R2 subpopulation in CCR1-deficient cells. Because the R1 and R2 subpopulations reportedly express higher and lower levels of RANK, respectively (29), a reduction in the R2 subpopulation likely contributed to reduced expression of osteoclast markers in CCR1-deficient osteoclastic cells. Importantly, our observation is also consistent with a previous work reporting that RANK^{lo} precursors are required for cellular fusion (29).

CCR1 Signaling Is Involved in Osteoclast Differentiation—To further explore the role of CCR1 signaling in osteoclast differentiation, we next examined the expression levels of chemokine receptors during osteoclastogenesis using an *in vitro* culture system. CCR1 was expressed in the course of the osteoclastogenesis, with the highest levels of expression at day 4 after culture (10–12), whereas other chemokine receptor CCR2 was gradually down-regulated during this culture period (30)

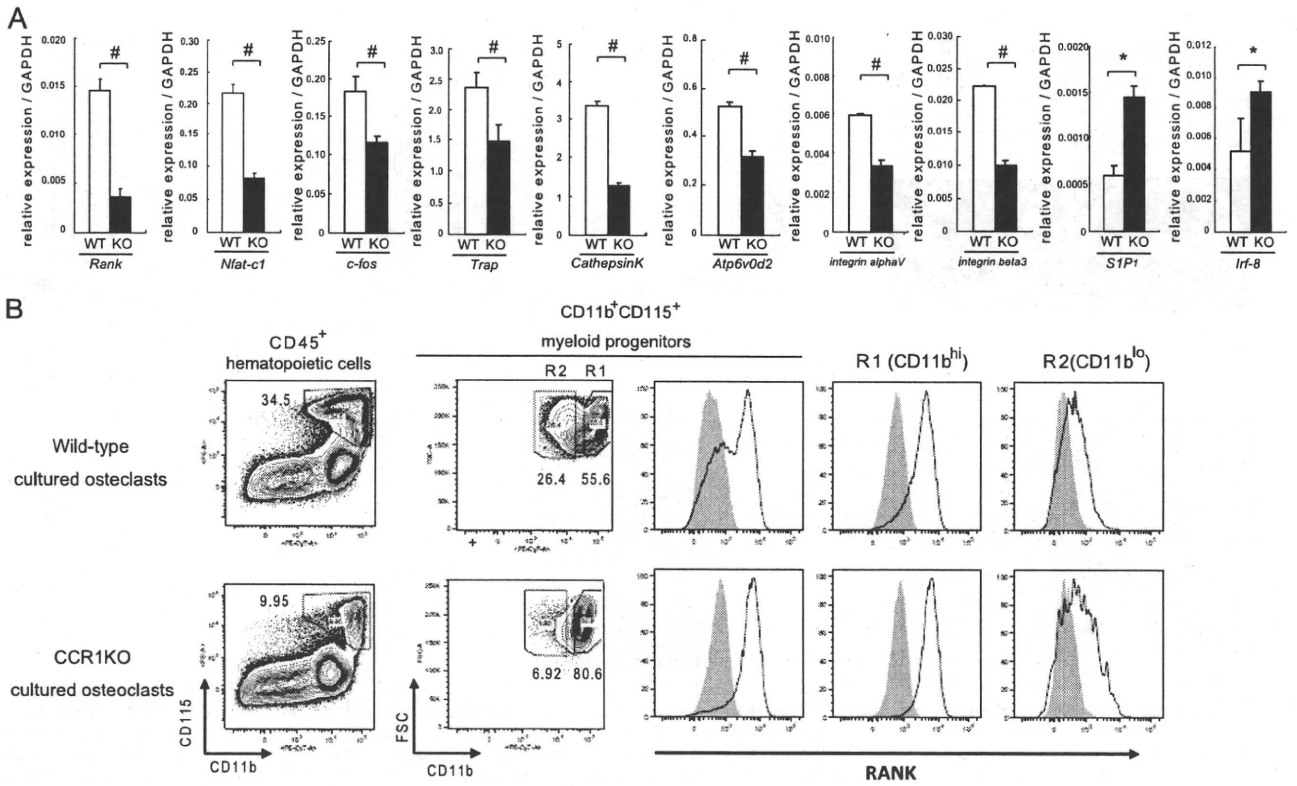

FIGURE 5. **Osteoclastic impairment by CCR1 deficiency is due to the changes in osteoclastic precursor population.** Pre-osteoclastic cells were cultured from the bone marrow of wild-type and *Ccr1*$^{-/-}$ mice. Osteoclasts were induced from the pre-osteoclastic cells by M-CSF and RANKL treatment. In *A*, relative expression levels of the osteoclastic differentiation markers (*Rank*, *Nfatc1* transcription factor, *c-fos*, *Trap*, *CathepsinK* protease, H^+-ATPase subunit *ATP6v0d2*, integrins αV and $\beta 3$, *S1P*$_1$, and *Irf-8*) on wild-type (*open column*) and *Ccr1*$^{-/-}$ (*filled column*) osteoclasts were measured by a real-time Q-PCR analysis at day 4 after culture (mean ± S.E., $n = 5$). #, significantly different from wild-type controls, $p < 0.05$. In *B*, expression analysis of RANK in $CD45^+CD11b^+CD115^+$ pre-osteoclastic cells isolated from the bone marrows of wild-type and *Ccr1*$^{-/-}$ mice after 4 days in culture were analyzed by flow cytometry.

(Fig. 6*A*). Immunohistochemical staining revealed that CCR1 was highly expressed on the multinuclear osteoclasts (supplemental Fig. 3). The expression profiles of CCR ligands in this *in vitro* osteoclast culture system revealed that ligands specific for CCR1, such as *Ccl5* and *Ccl9*, had a relatively higher levels of expression than other ligands, and appeared to be regulated depending on the maturation stages of the osteoclasts. *Ccl5* was preferentially expressed at day 4, a stage of mononuclear pre-osteoclasts, whereas multinuclear osteoclasts predominantly produced *Ccl9* at later times (Fig. 6*B*). These regulated transcriptional patterns of *Ccl5* and *Ccl9* were also confirmed by the analysis of protein expression levels in cultured media (Fig. 6*C*). These observations suggested that the interaction between CCR1 and its ligands, CCL5 and CCL9, could be involved in osteoclast differentiation.

We verified this hypothesis by culturing osteoclast precursors in the presence of neutralizing antibodies against CCL5 and CCL9. Blockade of either ligand resulted in a partial inhibition of osteoclast formation in a dose-dependent manner. Similarly, simultaneous treatment with neutralizing antibodies against CCL5 and CCL9 induced synergistic inhibitory effects (Fig. 6*D*). Furthermore, PTX treatment blocked osteoclastogenesis to the basal levels. Notably, we found no CCL3 production by ELISA or any inhibitory osteoclastogenesis effects using an anti-CCL3 antibody (data not shown), although CCL3 is thought to play an essential role in inflammation-related osteoclastogenesis in humans (4, 7, 31, 32). These findings indicate that CCR1 is essential for osteoclast differentiation, and CCL5 and CCL9 are the likely candidate ligands that participate in the CCR1 axis.

CCR1 Is Involved in the RANK–RANKL Axis and Induces the Impaired Osteoclastogenesis—Because osteoclast differentiation is critically regulated by the signals through the RANK–RANKL axis, we investigated the transcriptional level of *Rankl* in *Ccr1*$^{-/-}$ osteoblastic cells. The cells expressed significantly lower levels of RANKL compared with wild-type osteoblastic cells (Fig. 7*A*). We next performed co-cultures of pre-osteoclasts with layers of osteoblastic cells by reciprocal combinations of these two cell populations from wild-type and *Ccr1*$^{-/-}$ mice. As expected from the reduced *Rankl* expression, a significantly reduced number of osteoclasts were formed from co-culture with *Ccr1*$^{-/-}$ osteoblastic cells compared with wild-type osteoblastic cells (Fig. 7*B*). In the presence of PTX, wild-type osteoblastic cells also failed to generate substantial numbers of osteoclasts (Fig. 7*B*). *Ccr1*$^{-/-}$ osteoclast precursors did not form differentiated osteoclasts even in the presence of wild-type-derived osteoblasts (Fig. 7*C*), as is consistent with our observations in Fig. 4. These observations suggest that the CCR1 chemokine receptor, which is expressed by both osteoblasts and osteoclasts, plays a critical role on osteoblast-osteoclast communication through the regulation of the RANK and RANKL expression.

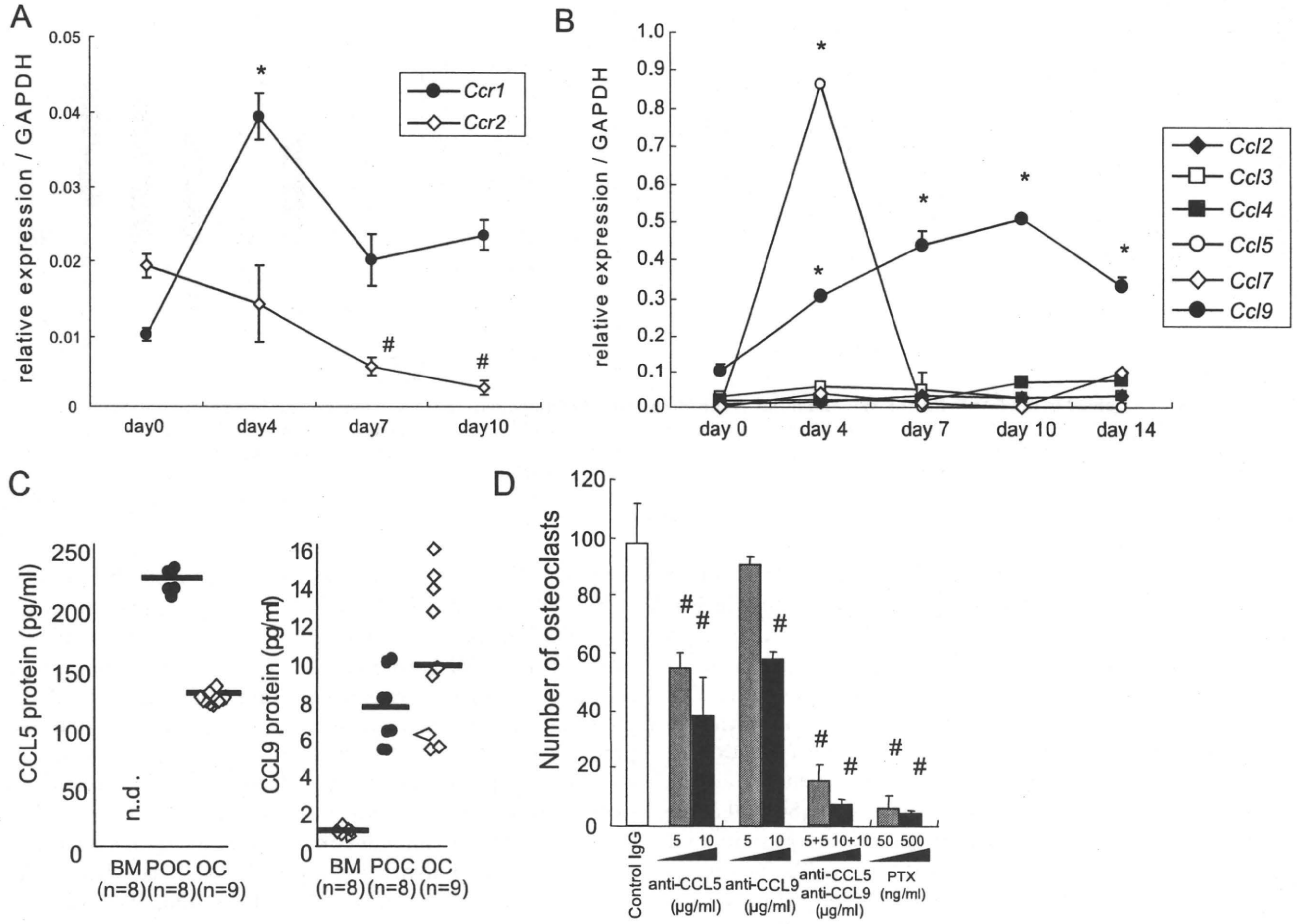

FIGURE 6. **CCR1 signaling is involved in osteoclast differentiation.** Osteoclastic cells and macrophages were cultured from the bone marrow of wild-type and *Ccr1*$^{-/-}$ mice. Total RNAs were isolated from the cultured cells. The relative mRNA expression levels of chemokine receptors *Ccr1*, *Ccr2* (*A*) and chemokine ligands (*B*) during osteoclastogenesis were measured by real-time Q-PCR (mean ± S.E., $n = 5$). * and #, significantly different from day 0 of *Ccr1* and *Ccr2*, respectively, $p < 0.05$ in *A*. *, significantly different from day 0 of culture in each ligand expression, $p < 0.05$ in *B*. In *C*, chemokine levels during osteoclastogenesis were measured by ELISA. *BM*, bone marrow-derived macrophage; *POC*, pre-osteoclast (day 4); and *OC*, osteoclast (day14). *Bars* indicate the mean. In *D*, the number of osteoclasts after neutralization of CCL5, CCL9, and their combination in the osteoclastic cultures were scored (mean ± S.E., $n = 3$). #, significantly different between two distinct concentrations of each antibody, $p < 0.05$. *PTX*, pertussis toxin.

DISCUSSION

Pathological findings postulate that chemokines and chemokine receptors are involved in bone remodeling (9–13). Among these receptors, CCR1 appears to be an important molecule involved in bone metabolism (9). We used *Ccr1*$^{-/-}$ mice to investigate whether CCR1 affects bone metabolism. Our findings have demonstrated that a CCR1-deficiency affects the differentiation and function of both osteoblasts and osteoclasts, and also causes osteopenia.

Our bone histomorphometric study in *Ccr1*$^{-/-}$ mice clearly demonstrated impaired osteoblast differentiation and function (Fig. 1, *D–G*). The bone tissues in *Ccr1*$^{-/-}$ mice exhibited down-regulation of *osteocalcin*, which is a marker for mature osteoblasts, whereas the expression of *Osteonectin* and *Osteopontin*, which are markers for early osteoblasts, were up-regulated in the bones of these mice (Fig. 2*A*). Significantly, *Ccr1*$^{-/-}$ osteoblastic cells exhibited much less potency to generate mineralized tissues (Fig. 3*A*). These results suggest that the deficiency of CCR1 results in arrested osteoblast maturation and defective osteoblast function. Previous reports have demonstrated that the sustained expression of *Runx2* in osteoblasts inhibits their terminal maturation and causes osteopenia with a reduction in the number of osteocytes (25, 33). Consistent with these findings, bone tissue specimens from *Ccr1*$^{-/-}$ mice exhibited a higher expression level of *Runx2* and a reduced number of osteocytes (Fig. 3*G*). These findings suggest that osteopenia in *Ccr1*$^{-/-}$ mice is due to impaired osteoblastic function via *Runx2* up-regulation. Our findings in *Ccr1*$^{-/-}$ osteoblastic culture supportively demonstrated that an inverse temporal expression level of osteoblastic transcriptional factors, such as *Runx2*, *Atf4*, and *Osterix* could be related to the disordered expressions of bone matrix proteins, thus resulting in impaired bone mineral deposition (Fig. 3*B*).

Furthermore, treatment with neutralizing antibodies against CCR1 ligands (*e.g.* CCL4, CCL5, CCL9, and CCL11) significantly inhibited mineral deposition (Fig. 3*E*) and osteoblastic protein expression (supplemental Fig. 2) in osteoblastic cells isolated from wild-type mice. These observations indicate that CCR1-mediated signaling is essential for osteoblast differentiation and function. Although we detected substantial levels of

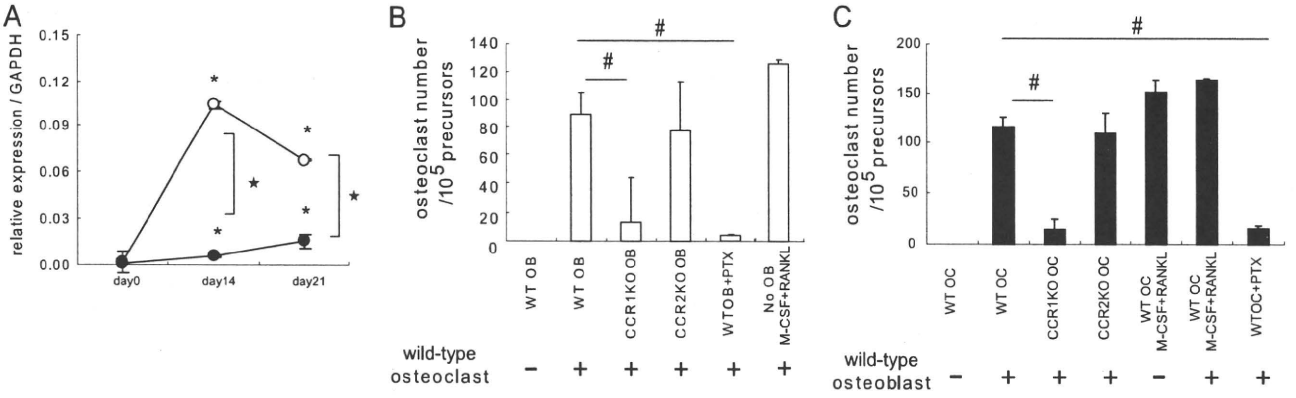

FIGURE 7. **CCR1 is involved in the RANK–RANKL axis and induces the impaired osteoclastogenesis.** In *A*, osteoblastic cells were cultured from the bone marrow of wild-type and $Ccr1^{-/-}$ mice. Relative expression levels of *Rankl* by $Ccr1^{-/-}$ osteoblasts as measured by real-time Q-PCR (mean ± S.E., $n = 3$). #, significantly different from wild-type controls, $p < 0.05$. In *B* and *C*, the number of $TRAP^+$ multinuclear osteoclasts induced by co-culture with osteoblasts. Co-culture with osteoblastic cells isolated from wild-type or $Ccr1^{-/-}$ mice (mean ± S.E., duplicated, $n = 2$, *B*), and with osteoclast precursors isolated from wild-type or $Ccr1^{-/-}$ mice (mean ± S.E., duplicated, $n = 2$, *C*). Osteoclast cultures with M-CSF and RANKL without osteoblasts were set as positive control. #, significantly different from co-culture of osteoclasts with wild-type osteoblasts, $p < 0.05$.

various chemokine ligands (CCL4, CCL5, CCL9, and CCL11) in osteoblastic cells, these levels were greatly reduced in cells isolated from $Ccr1^{-/-}$ mice (Fig. 3*D*). This observation implies a chemokine-dependent amplification loop by which a given chemokine signaling sustains or amplifies the expressions of its participating ligands and receptors, which has been previously reported in several contexts. For instance, the activation of $CD14^+$ monocytes form a CCR2-CCL2 axis-dependent amplification loop that ultimately leads to fibrosis (34). Several other studies have reported that macrophage infiltration in injured tissue is mediated by a CCR1-mediated loop (35–37) and a CCR5–CCL5 loop (38). Reports of renal inflammatory signals and abdominal inflammation have described CCR7–CCL19/CCL21 (39) and CCR8–CCL1 loops (17), respectively. Therefore, the CCR1-mediated loop is likely to be involved in osteoblast differentiation, function, and cellular interactions that regulate bone metabolism. Possible roles of the CCR1-mediated loop in osteoblast differentiation and function suggest that changes in the bone marrow microenvironment by a CCR1 deficiency affected the osteoblastic lineage and/or the intercellular regulation of osteoblast differentiation and function. CCR1 conventional knock-down seems to have affected many cell types that express CCR1, affecting the bone marrow microenvironment, which regulates whole process of osteoblast differentiation and function. Our *in vitro* experiments did not successfully retrieve this point. Nevertheless, the present experiments have confirmed an essential role for CCR1-mediated signaling in osteoblastic cells. The expression and possible roles of CCR1 in osteoclast lineage cells have been reported by several studies (4, 10, 11). We observed the up-regulation of *Ccr1* expression and down-regulation of *Ccr2* during cultured osteoclastogenesis (Fig. 6*A*). The bone histomorphometric analyses demonstrated impaired osteoclast differentiation and function in $Ccr1^{-/-}$ mice (Fig. 1*F*). In addition, we observed impaired bone resorption activity by osteoclasts isolated from $CCR1^{-/-}$ mice (Fig. 4, *B* and *C*). A potential reason for the impaired bone resorption is due to defects in osteoclast differentiation. Indeed, the flow cytometric analyses revealed that the component of $CD11b^+CD115^+$ myeloid-lineage precursors in $Ccr1^{-/-}$ mice are drastically changed; this population of cells lacked the $RANK^{lo}$ $CD11b^{lo}$ subpopulation, which is required for cellular fusion (29) (Fig. 5*B*). Recent live observation of calvarial bone marrow by two-photon microscopy clarified the roles of chemoattractant $S1P_1$ (sphingosine-1-phosphate 1) and its receptors in the migration of osteoclast precursors to the bone surface (40). Therefore, it is indeed intriguing to speculate that elevated levels of $S1P_1$ expression in $Ccr1^{-/-}$ osteoclasts (Fig. 1*F*) reduced the supply of osteoclast precursors from peripheral circulation in the bone marrow to the bone surface. Further investigation will reveal whether the CCR1 axis is involved in the chemotactic migration of osteoclast precursors to the bone surface.

One of the possible reasons for osteoclast dysfunction in $Ccr1^{-/-}$ mice may be diminished signaling along the RANK–RANKL axis. The down-regulation of both *Rank* and *Rankl* mRNA was observed in the bone tissue of $Ccr1^{-/-}$ mice (Fig. 2*D*). Cultured osteoblastic cells and osteoclasts isolated from $Ccr1^{-/-}$ mice exhibited remarkable reductions in *Rank* and *Rankl* expression levels, respectively (Figs. 5*B* and 7*B*). Furthermore, *Ccr1*-deficient osteoclasts had discouraged the levels of osteoclastic maturation markers such as *c-fos*, *Nfatc1*, *CathepsinK*, and several integrins (Fig. 5*A*). These results suggest that CCR1-mediated signaling controls the RANK–RANKL axis through the regulation of both osteoblasts and osteoclasts. Our intercross co-cultures of pre-osteoclasts with osteoblastic cells from wild-type and $Ccr1^{-/-}$ mice obviously demonstrated an impaired interaction between these two cell types, resulting in the impaired induction of functional mature osteoclasts (Fig. 7, *B* and *C*). These findings, interestingly, support the idea that the chemokines produced by the osteoblasts and osteoclasts that stimulate CCR1-mediated signaling could be categorized as putative "bone-coupling factors" (41), which mediate the cross-talk between osteoclasts and osteoblasts to maintain bone remodeling.

Our data imply that the regulatory mechanism of *Rankl* expression is associated with osteoblast maturation. Runx2 reportedly induce a low steady-state level of *Rankl* expression and is also required for the stimulatory effect of vitamin

D_3 on *Rankl* transcription possibly by condensing or decondensing the chromatin structure (42). It is possible that the inverse-temporal *Runx2* expression in CCR1-deficient mice is causative of the down-regulation of *Rankl*, due to a reduced cellular response to bone-targeted hormones such as vitamin D_3 and parathyroid hormone. However, a more direct role of CCR1-mediated signaling on *Rankl* transcription remains to be elucidated.

CCR1-mediated signaling pathways on both osteoblasts and osteoclasts raise important questions on how the several members of murine chemokine ligands for CCR1 (in rodents, CCL3, CCL4, CCL5, CCL6, CCL8, CCL9, and CCL11) (43) distinguish the downstream signaling pathways, despite sharing the same CCR1 receptor. Each chemokine may possess specific regulatory control for binding to the receptor and inducing a specific cellular response. For example, the osteoclasts may have a distinct intrinsic signaling adaptor protein for cellular response, as well as the adaptor protein FROUNT for CCR2-mediated signaling (44). It has also been demonstrated that the spatiotemporal expression of chemokine receptors and their ligands may relay chemokine signaling and sequential output that regulate bone metabolism. This is related to several findings in this study, including the distinct temporal expression patterns of different ligands as observed in Fig. 6 (*B* and *C*) and supplemental Fig. 1, the chemokine-dependent amplification loop, and the possible chemokine-mediated cellular interaction. Further studies are warranted to investigate the intracellular signaling pathways downstream of each chemokine receptor.

Our current results also support the concept that chemokine receptor antagonists are potentially novel therapeutic candidates for the treatment of patients with certain inflammatory bone diseases. Several reports suggest that CCL3 promotes pathological bone destruction by excessively triggering osteoclast activation (2, 4, 7, 31, 32). However, we were unable to detect increased CCL3 production by cultured osteoclasts (Fig. 6, *B* and *C*, and data not shown), suggesting that physiological osteoclastogenesis is primarily maintained by CCL9 rather than CCL3. It is probable that pro-inflammatory CCL3 overcomes the physiological process of osteoclastogenesis by CCL9 expression and signaling, thereby inducing ectopic osteoclastogenesis that causes bone destruction mediated by T-lymphocyte-mediated activation (45). Alternatively, the species differences between rodents and humans must be considered; CCL9 is described only in rodents, and the putative human homologue is predicted to be CCL15 and CCL23 (46), which are potent osteoclastogenesis mediators in humans (47). It is therefore worthwhile to dissect the distinct roles of chemokine signaling in both the pathological and physiological contexts, which would provide novel information that may help researchers identify new therapeutic targets.

In conclusion, the present observations provide the first evidence for the physiological roles of CCR1-mediated chemokines in the bone metabolism. Further studies on chemokine receptors in the bone metabolism will enable the targeted development of new therapeutic strategies for the treatment of patients with bone destruction diseases and osteoporosis.

Acknowledgments—We thank Dr. Taeko Dohi, Dr. Harumi Suzuki, Dr. Yasuhiro Natori, and Mikiko Uwano (International Medical Center of Japan (IMCJ)), Dr. Philip M. Murphy (NIH), Dr. Tomoki Nakashima (Tokyo Medical and Dental University), and T. Sakai for valuable advices and supports. The authors are grateful to Dr. Takuro Shimbo and Dr. Tetsuya Mizoue (IMCJ) for statistical support.

REFERENCES

1. Charo, I. F., and Ransohoff, R. M. (2006) *N. Engl. J. Med.* **354,** 610–621
2. Oba, Y., Lee, J. W., Ehrlich, L. A., Chung, H. Y., Jelinek, D. F., Callander, N. S., Horuk, R., Choi, S. J., and Roodman, G. D. (2005) *Exp. Hematol.* **33,** 272–278
3. Kim, M. S., Magno, C. L., Day, C. J., and Morrison, N. A. (2006) *J. Cell Biochem.* **97,** 512–518
4. Menu, E., De Leenheer, E., De Raeve, H., Coulton, L., Imanishi, T., Miyashita, K., Van Valckenborgh, E., Van Riet, I., Van Camp, B., Horuk, R., Croucher, P., and Vanderkerken, K. (2006) *Clin. Exp. Metastasis* **23,** 291–300
5. Haringman, J. J., Smeets, T. J., Reinders-Blankert, P., and Tak, P. P. (2006) *Ann. Rheum. Dis.* **65,** 294–300
6. Choi, S. J., Cruz, J. C., Craig, F., Chung, H., Devlin, R. D., Roodman, G. D., and Alsina, M. (2000) *Blood* **96,** 671–675
7. Han, J. H., Choi, S. J., Kurihara, N., Koide, M., Oba, Y., and Roodman, G. D. (2001) *Blood* **97,** 3349–3353
8. Vallet, S., Raje, N., Ishitsuka, K., Hideshima, T., Podar, K., Chhetri, S., Pozzi, S., Breitkreutz, I., Kiziltepe, T., Yasui, H., Ocio, E. M., Shiraishi, N., Jin, J., Okawa, Y., Ikeda, H., Mukherjee, S., Vaghela, N., Cirstea, D., Ladetto, M., Boccadoro, M., and Anderson, K. C. (2007) *Blood* **110,** 3744–3752
9. Yang, M., Mailhot, G., MacKay, C. A., Mason-Savas, A., Aubin, J., and Odgren, P. R. (2006) *Blood* **107,** 2262–2270
10. Yu, X., Huang, Y., Collin-Osdoby, P., and Osdoby, P. (2004) *J. Bone Miner. Res.* **19,** 2065–2077
11. Lean, J. M., Murphy, C., Fuller, K., and Chambers, T. J. (2002) *J. Cell Biochem.* **87,** 386–393
12. Okamatsu, Y., Kim, D., Battaglino, R., Sasaki, H., Spate, U., and Stashenko, P. (2004) *J. Immunol.* **173,** 2084–2090
13. Kominsky, S. L., Abdelmagid, S. M., Doucet, M., Brady, K., and Weber, K. L. (2008) *Cancer Res.* **68,** 1261–1266
14. Binder, N. B., Niederreiter, B., Hoffmann, O., Stange, R., Pap, T., Stulnig, T. M., Mack, M., Erben, R. G., Smolen, J. S., and Redlich, K. (2009) *Nat. Med.* **15,** 417–424
15. Gao, J. L., Wynn, T. A., Chang, Y., Lee, E. J., Broxmeyer, H. E., Cooper, S., Tiffany, H. L., Westphal, H., Kwon-Chung, J., and Murphy, P. M. (1997) *J. Exp. Med.* **185,** 1959–1968
16. Doi, M., Nagano, A., and Nakamura, Y. (2002) *Biochem. Biophys. Res. Commun.* **290,** 381–390
17. Hoshino, A., Kawamura, Y. I., Yasuhara, M., Toyama-Sorimachi, N., Yamamoto, K., Matsukawa, A., Lira, S. A., and Dohi, T. (2007) *J. Immunol.* **178,** 5296–5304
18. Ito, M., Ikeda, K., Nishiguchi, M., Shindo, H., Uetani, M., Hosoi, T., and Orimo, H. (2005) *J. Bone Miner. Res.* **20,** 1828–1836
19. Parfitt, A. M., Drezner, M. K., Glorieux, F. H., Kanis, J. A., Malluche, H., Meunier, P. J., Ott, S. M., and Recker, R. R. (1987) *J. Bone Miner. Res.* **2,** 595–610
20. Liotta, L. A., and Stetler-Stevenson, W. G. (1990) *Semin. Cancer Biol.* **1,** 99–106
21. Gogly, B., Groult, N., Hornebeck, W., Godeau, G., and Pellat, B. (1998) *Anal. Biochem.* **255,** 211–216
22. Wilson, M. J., Strasser, M., Vogel, M. M., and Sinha, A. A. (1991) *Biol. Reprod.* **44,** 776–785
23. Komori, T., Yagi, H., Nomura, S., Yamaguchi, A., Sasaki, K., Deguchi, K., Shimizu, Y., Bronson, R. T., Gao, Y. H., Inada, M., Sato, M., Okamoto, R., Kitamura, Y., Yoshiki, S., and Kishimoto, T. (1997) *Cell* **89,** 755–764
24. Ducy, P., Zhang, R., Geoffroy, V., Ridall, A. L., and Karsenty, G. (1997) *Cell* **89,** 747–754

25. Liu, W., Toyosawa, S., Furuichi, T., Kanatani, N., Yoshida, C., Liu, Y., Himeno, M., Narai, S., Yamaguchi, A., and Komori, T. (2001) *J. Cell Biol.* **155,** 157–166
26. Delmas, P. D. (1993) *J. Bone Miner. Res.* **8,** Suppl. 2, S549–S555
27. Takahashi, M., Kushida, K., Hoshino, H., Ohishi, T., and Inoue, T. (1997) *J. Endocrinol. Invest* **20,** 112–117
28. Schneider, D. L., and Barrett-Connor, E. L. (1997) *Arch. Intern. Med.* **157,** 1241–1245
29. Arai, F., Miyamoto, T., Ohneda, O., Inada, T., Sudo, T., Brasel, K., Miyata, T., Anderson, D. M., and Suda, T. (1999) *J. Exp. Med.* **190,** 1741–1754
30. Saitoh, Y., Koizumi, K., Sakurai, H., Minami, T., and Saiki, I. (2007) *Biochem. Biophys. Res. Commun.* **364,** 417–422
31. Abe, M., Hiura, K., Wilde, J., Moriyama, K., Hashimoto, T., Ozaki, S., Wakatsuki, S., Kosaka, M., Kido, S., Inoue, D., and Matsumoto, T. (2002) *Blood* **100,** 2195–2202
32. Chintalacharuvu, S. R., Wang, J. X., Giaconia, J. M., and Venkataraman, C. (2005) *Immunol. Lett.* **100,** 202–204
33. Kanatani, N., Fujita, T., Fukuyama, R., Liu, W., Yoshida, C. A., Moriishi, T., Yamana, K., Miyazaki, T., Toyosawa, S., and Komori, T. (2006) *Dev. Biol.* **296,** 48–61
34. Sakai, N., Wada, T., Furuichi, K., Shimizu, K., Kokubo, S., Hara, A., Yamahana, J., Okumura, T., Matsushima, K., Yokoyama, H., and Kaneko, S. (2006) *J. Leukoc. Biol.* **79,** 555–563
35. Furuichi, K., Gao, J. L., Horuk, R., Wada, T., Kaneko, S., and Murphy, P. M. (2008) *J. Immunol.* **181,** 8670–8676
36. Ma, B., Zhu, Z., Homer, R. J., Gerard, C., Strieter, R., and Elias, J. A. (2004) *J. Immunol.* **172,** 1872–1881
37. Shang, X., Qiu, B., Frait, K. A., Hu, J. S., Sonstein, J., Curtis, J. L., Lu, B., Gerard, C., and Chensue, S. W. (2000) *Am. J. Pathol.* **157,** 2055–2063
38. Anders, H. J., Frink, M., Linde, Y., Banas, B., Wörnle, M., Cohen, C. D., Vielhauer, V., Nelson, P. J., Gröne, H. J., and Schlöndorff, D. (2003) *J. Immunol.* **170,** 5658–5666
39. Coates, P. T., Colvin, B. L., Ranganathan, A., Duncan, F. J., Lan, Y. Y., Shufesky, W. J., Zahorchak, A. F., Morelli, A. E., and Thomson, A. W. (2004) *Kidney Int.* **66,** 1907–1917
40. Ishii, M., Egen, J. G., Klauschen, F., Meier-Schellersheim, M., Saeki, Y., Vacher, J., Proia, R. L., and Germain, R. N. (2009) *Nature* **458,** 524–528
41. Matsuo, K., and Irie, N. (2008) *Arch. Biochem. Biophys.* **473,** 201–209
42. Kitazawa, R., Mori, K., Yamaguchi, A., Kondo, T., and Kitazawa, S. (2008) *J. Cell Biochem.* **105,** 1289–1297
43. Murphy, P. M., Baggiolini, M., Charo, I. F., Hébert, C. A., Horuk, R., Matsushima, K., Miller, L. H., Oppenheim, J. J., and Power, C. A. (2000) *Pharmacol. Rev.* **52,** 145–176
44. Terashima, Y., Onai, N., Murai, M., Enomoto, M., Poonpiriya, V., Hamada, T., Motomura, K., Suwa, M., Ezaki, T., Haga, T., Kanegasaki, S., and Matsushima, K. (2005) *Nat. Immunol.* **6,** 827–835
45. Sato, K., Suematsu, A., Okamoto, K., Yamaguchi, A., Morishita, Y., Kadono, Y., Tanaka, S., Kodama, T., Akira, S., Iwakura, Y., Cua, D. J., and Takayanagi, H. (2006) *J. Exp. Med.* **203,** 2673–2682
46. Votta, B. J., White, J. R., Dodds, R. A., James, I. E., Connor, J. R., Lee-Rykaczewski, E., Eichman, C. F., Kumar, S., Lark, M. W., and Gowen, M. (2000) *J. Cell Physiol.* **183,** 196–207
47. Rioja, I., Hughes, F. J., Sharp, C. H., Warnock, L. C., Montgomery, D. S., Akil, M., Wilson, A. G., Binks, M. H., and Dickson, M. C. (2008) *Arthritis Rheum* **58,** 2257–2267

2．歯科口腔外科の立場から

国立国際医療研究センター病院　歯科口腔外科　丸岡　豊

[はじめに]

ビスフォスフォネート剤関連顎骨壊死(BRONJ: Bisphosphonate Related Osteonecrosis of the Jaw）は、骨粗鬆症や悪性疾患等に対して処方されたビスフォスフォネート剤（以下BP剤）を使用している患者に起こる極めて難治性の症状である（写真１）。

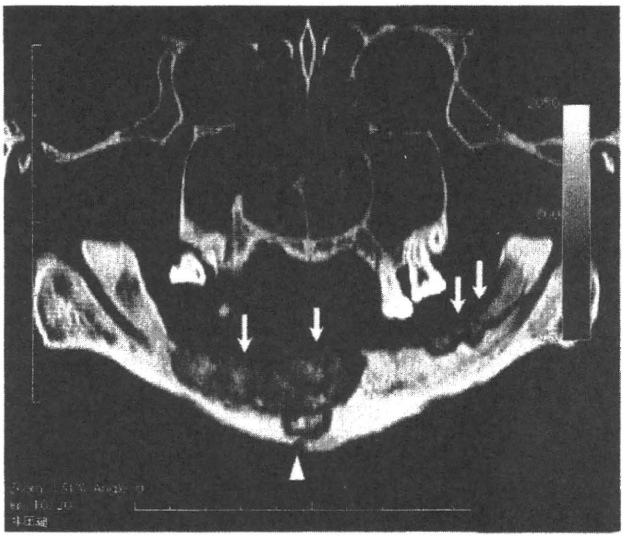

写真１：BRONJを発症した下顎骨のCT再構成写真（50代　男性）
↓で示した部分に辺縁不整な白い綿状にみえる壊死骨が遊離している。周囲の下顎骨も高濃度を示しており、BP剤使用による骨のリモデリングの抑制による硬化を疑わせる。オトガイ部には病的骨折を起こしている状態が観察できる（△）。

抜歯などの骨に侵襲を伴う治療が誘因とされるが、投与されている薬剤・局所的因子・身体的因子・遺伝的因子など様々な要因が複雑に絡み、発症のメカニズムは未だ不明である。発症確率は0.8～12%と推定されるが、本疾患の認知の増加、ならびに投与期間や追跡期間の延長に伴い、発生頻度はむしろ増えている。一旦発症すると顎骨骨髄炎様症状を呈し、疼痛や機能障害に苦しむばかりでなく、軟組織及び硬組織の感染巣を抱えることになるため、原病の治療計画にも重大な影響を及ぼす。

現在、BRONJの予防法や対処法が確立されているとは言いがたい。そこでその予防や対応策の一助となるべく、「ビスフォスフォネート関連顎骨壊死検討委員会」から統一的見解としてポジションペーパーが出されている[1]。本発表ではそれに沿ってBRONJの概要に触れるとともに、その対策などを考えていきたい。

[顎骨壊死の原因]

全身の骨の中でなぜ顎骨だけに骨壊死が発症するのかは未だに不明であるが、図１に示すような理由が考えられている。

・歯と歯肉の隙間から、細菌が顎骨に侵入しやすい。
・薄い粘膜にしか守られていない骨は他にはなく、食事などの日常生活において傷害を受けやすい。
・もともと口の中には常在菌が極めて多い。
・下顎骨は上顎骨などに比べて緻密で、BP剤が蓄積しやすい。
・むし歯や歯周病を通じて、顎骨に病変が伝わりやすい。
・抜歯などの治療により、顎骨が直接口の中に現れやすい。

図１：顎骨の特殊性（文献１より引用）

BP剤には多くの種類があり、その側鎖に窒素を含有しているBP剤の方がBRONJを起こしやすいといわれている。また骨吸収抑制作用が一般的に強いためでもあろうが、注射薬の方が経口薬よりもリスクが高いといわれている。

図２に国立国際医療研究センター病院の診療科別の経口BP剤の処方患者数を示すが、15年間で実に1811名の患者にBP剤が処方されている。整形外科やステロイドを使用することの多い膠原病内科、呼吸器内科からの処方が多いことがわかる。しかし、ほぼ全科から処方がされていることから考えると、本剤が「安全な薬剤」という認識で処方されている（あるいは、「いた」）ことがわかる。当院における経口BP剤に関するBRONJの罹患率は、10万人年あたり35.7であった。他科の患者を全て追跡できていないにもかかわらず、報告されているよりも35～50倍近く高かった。

参考までに報告されているBRONJ発症リスクは

欧州骨粗鬆症WG（2009）：10万人年あたり1件未満（経口剤）
10万人年あたり95件（注射剤）[2]
米国口腔外科学会（2009）：10万人年あたり0.7件（経口剤）
累積発現頻度0.8～12%（注射剤）[3]

である。

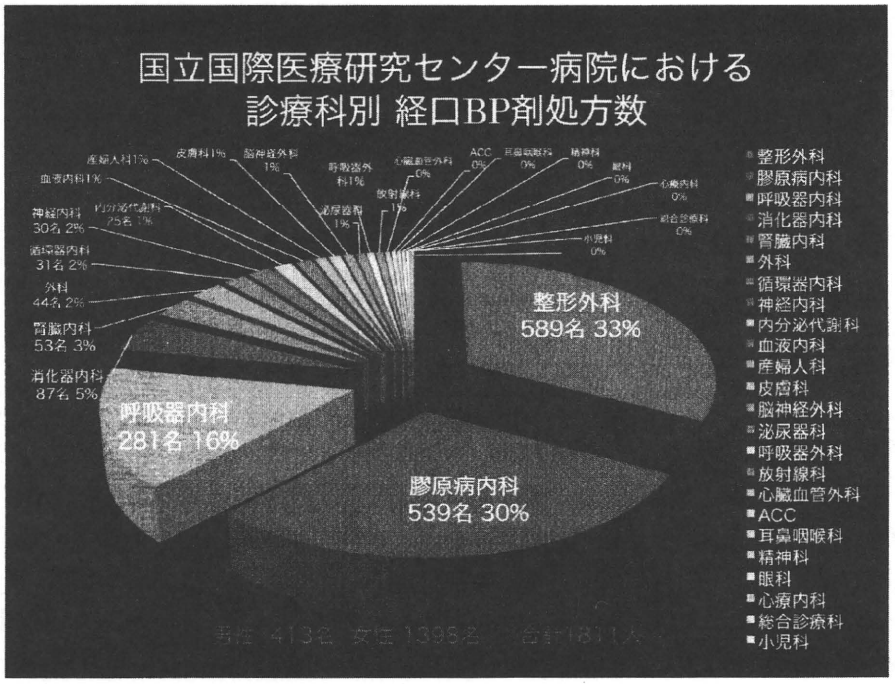

図２：国立国際医療研究センター病院における1995年から2009年までの経口BP剤の診療科別処方患者数（名）

一方、局所的ファクターとしては、喫煙や抜歯、歯科インプラント埋入、根尖外科手術、歯周外科手術などの侵襲的歯科治療、歯周病などが挙げられている。

[BRONJ患者の歯科治療]

可能であれば，すべての歯科治療を終えた後にBP剤を投与するのが望ましいが、現実的にはそれを完全に遂行することは困難である。

一般的に問題ないと思われているのは、通常のむし歯の治療、浅い歯石の除去やクリーニング、神経を取る治療（歯内治療）、義歯治療などである。しかしその一方、前述のごとく抜歯や歯科用インプラント、深い位置まで及ぶ歯周病の治療、すなわち顎骨が露出する等の侵襲的歯科治療には注意が必要と思われる。

昨年までは、注射用BP剤投与中の患者に対しては，侵襲的歯科治療を行わない、そして３か月間のBP剤の休薬を行えばBRONJ発生が予防できる、とされていた。しかし、2010年のポジションペーパーではBP剤の休薬がBRONJ発生を予防するという明らかな臨床的エビデンスはない、とされている。さらに注射用BP剤投与中の患者に対しては，侵襲的歯科治療を行うことの是非について明らかな見解は得られていない。つまり注射用BP剤投与中の患者には、BP剤のリスクと治療効果を勘案して、原則的にBP剤投与を継続して、侵襲的歯科治療はできるかぎり避ける、とされた（図３）。すなわち、結果としてBP剤の投与中止は不要であるということになる。